

On the Systematic Measurement Errors of Correlative Mobile Radio Channel Sounders

Gerald Matz, *Member, IEEE*, Andreas F. Molisch, *Senior Member, IEEE*, Franz Hlawatsch, *Senior Member, IEEE*, Martin Steinbauer, *Student Member, IEEE*, and Ingo Gaspard

Abstract—We show that measurements of time-varying mobile radio channels obtained with uncalibrated correlative channel sounders are affected by four different types of systematic errors (commutation, pulse-compression, aliasing, and misinterpretation error). We analyze these errors and provide upper error bounds that are formulated in terms of channel and sounder parameters. Based on these error bounds, we provide guidelines for a judicious choice of important sounder parameters. Computer simulations using a simple two-path channel illustrate our theoretical results. Finally, we show how our results can be used to assess the accuracy of measured channel data.

Index Terms—Channel measurements, channel sounder, mobile radio channels, time-varying channels.

I. INTRODUCTION

ACCURATE measurements of mobile radio channels are vital for the design, simulation, and performance evaluation of mobile radio systems [1]. Due to higher data rates and multiple access techniques, most wireless systems are wideband [2]. Thus, it has become necessary and common to use wideband channel sounders [3]–[6].

There are essentially three popular types of channel sounders [4]–[6]: 1) pseudonoise (PN) sequence correlation sounders; 2) swept time-delay cross-correlation sounders; and 3) chirp sounders.¹ These sounders are based on correlation/pulse-compression techniques and on the assumption that the channel does not change during a measurement period, i.e., that it is quasi-time-invariant (quasi-static). However, increasingly higher carrier frequencies result in larger Doppler shifts and thus in faster channel variations. These channel variations cause several different types of systematic errors in the sounder measurements.

Unfortunately, the usual rule of thumb—namely, that the channel can be viewed as effectively time-invariant if the

sounding period is much smaller than the reciprocal of the maximum Doppler shift—does not provide a *quantitative* characterization of the measurement errors actually incurred during a specific measurement campaign. In this paper, we will show that the total measurement error consists of four different components, and we will provide a quantitative analysis of each error component in terms of upper error bounds. These error bounds are practically useful since they allow to assess the accuracy of measured channel data and provide guidelines for a judicious choice of sounder parameters.

It appears that only one of the systematic errors to be discussed here has been recognized in the past. This error is not due to time variations of the channel but to imperfect correlation/pulse-compression properties of the transmit and receive filters. Practical channel sounders often attempt to compensate for this error via *back-to-back calibration*. While calibrated sounders are not considered in this paper, we showed in [7] that in the case of time-varying channels conventional calibration suffers from systematic errors as well. In [7], an improved calibration method that is more immune to time variations is also proposed.

The rest of this paper is organized as follows. Section II briefly reviews some relevant channel descriptions. Section III presents a unified mathematical formulation of popular correlative channel sounding techniques. Section IV shows the existence of four types of systematic measurement errors of correlative channel sounders in the case of time-varying channels. Section V develops bounds on these errors. Guidelines for a judicious choice of important sounder parameters are provided in Section VI. Finally, in Section VII our theoretical findings are illustrated by computer simulations and their use in assessing the accuracy of measured channel data is demonstrated.

II. CHARACTERIZATION OF MOBILE RADIO CHANNELS

In this section, we review some descriptions of mobile radio channels. Fig. 1(a) shows a block diagram of the channel considered. It consists of a modulator (carrier frequency f_c), an ideal transmitter bandpass filter (bandwidth B), a time-varying RF link $\tilde{\mathbf{H}}$ (localized about f_c and not necessarily bandlimited), a receiver bandpass filter (again ideal with bandwidth B), and a demodulator. These system components are subsumed by an equivalent bandlimited complex baseband channel \mathbf{H} . The time-varying transfer functions (to be defined further below) of the radio link $\tilde{\mathbf{H}}$ and the equivalent baseband channel \mathbf{H} are shown in Fig. 1(b) and (c), respectively.

Paper approved by R. A. Valenzuela, the Editor for Transmission Systems of the IEEE Communications Society. Manuscript received July 28, 2000; revised November 14, 2000. This work was supported by EU Project META-MORP (SMT4-CT96-2093) and by FWF under Grant P11904-TEC and Grant P12228-TEC. This work was presented in part at IEEE VTC Fall 1999.

G. Matz, F. Hlawatsch, and M. Steinbauer are with the Institute of Communications and Radio-Frequency Engineering, Vienna University of Technology, A-1040 Vienna, Austria.

A. F. Molisch is with AT&T Labs Research, Middletown, NJ 07748 USA.

I. Gaspard is with Wide Area Radio Networks, T-Nova Deutsche Telekom InnovationsgesmbH, D64295 Darmstadt, Germany.

Publisher Item Identifier S 0090-6778(02)05113-9.

¹A fourth popular type is the frequency-sweep sounder that is based on a network analyzer. This sounder will not be considered here as it requires the channel to stay time-invariant for several seconds.

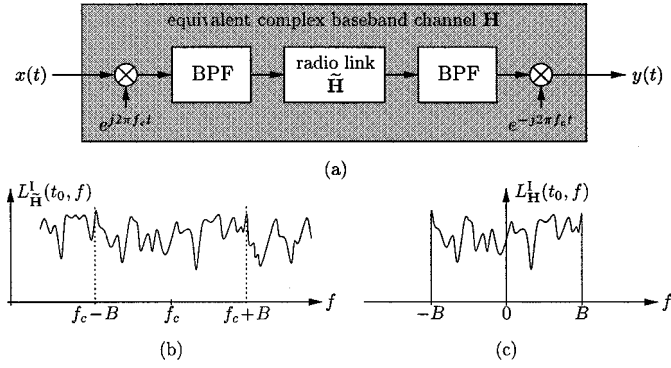


Fig. 1. Equivalent complex baseband model for a mobile radio channel. (a) Block diagram. (b) Time-varying transfer function of radio link \mathbf{H} at time t_0 . (c) Time-varying transfer function of equivalent baseband channel \mathbf{H} at time t_0 .

A. System Functions

The equivalent complex baseband channel \mathbf{H} is a linear, time-varying (LTV) system. This LTV system can be characterized by its kernel $k_{\mathbf{H}}(t, t')$ that relates the input $x(t)$ and the output $y(t)$ [see Fig. 1(a)] as²

$$y(t) = (\mathbf{H}x)(t) = \int_{t'} k_{\mathbf{H}}(t, t') x(t') dt'. \quad (1)$$

In mobile radio applications, the term *impulse response* usually refers to the channel's *input delay spread function* [8] defined as $h_{\mathbf{H}}^I(t, \tau) \triangleq k_{\mathbf{H}}(t, t - \tau)$. Alternatively, the *output delay spread function* [8] $h_{\mathbf{H}}^O(t, \tau) \triangleq k_{\mathbf{H}}(t + \tau, t)$ can be used. These functions are related by simple coordinate transforms

$$h_{\mathbf{H}}^I(t, \tau) = h_{\mathbf{H}}^O(t - \tau, \tau), \quad h_{\mathbf{H}}^O(t, \tau) = h_{\mathbf{H}}^I(t + \tau, \tau). \quad (2)$$

The Fourier transform of $h_{\mathbf{H}}^I(t, \tau)$ with respect to τ

$$L_{\mathbf{H}}^I(t, f) \triangleq \mathcal{F}_{\tau \rightarrow f} \{h_{\mathbf{H}}^I(t, \tau)\} = \int_{\tau} h_{\mathbf{H}}^I(t, \tau) e^{-j2\pi f \tau} d\tau$$

is referred to as *time-varying frequency response* or *time-varying transfer function* [8], [9]. It allows to rewrite the input–output relation (1) as

$$y(t) = \int_f L_{\mathbf{H}}^I(t, f) X(f) e^{j2\pi f t} df \quad (3)$$

where $X(f)$ denotes the Fourier transform of $x(t)$. The *frequency-dependent modulation function* [8]

$$L_{\mathbf{H}}^O(t, f) \triangleq \mathcal{F}_{\tau \rightarrow f} \{h_{\mathbf{H}}^O(t, \tau)\} = \int_{\tau} h_{\mathbf{H}}^O(t, \tau) e^{-j2\pi f \tau} d\tau \quad (4)$$

is an alternative definition of a time-varying transfer function. Both $L_{\mathbf{H}}^I(t, f)$ and $L_{\mathbf{H}}^O(t, f)$ are special cases of the *generalized Weyl symbol* [10] and reduce to the ordinary transfer function in the case of time-invariant systems. In [11]–[15], a transfer function calculus for the generalized Weyl symbol has been established; this calculus is closely related to our analysis of measurement errors in Section V.

²Unless indicated otherwise, integrals and sums are from $-\infty$ to ∞ .

The (*delay-Doppler* and *Doppler-delay*) *spreading functions* are defined as Fourier transforms of $h_{\mathbf{H}}^I(t, \tau)$ and $h_{\mathbf{H}}^O(t, \tau)$ with respect to t [8],

$$S_{\mathbf{H}}^I(\tau, \nu) \triangleq \int_t h_{\mathbf{H}}^I(t, \tau) e^{-j2\pi \nu t} dt \quad (5)$$

$$S_{\mathbf{H}}^O(\tau, \nu) \triangleq \int_t h_{\mathbf{H}}^O(t, \tau) e^{-j2\pi \nu t} dt. \quad (6)$$

They quantify the delays (time shifts) τ and Doppler (frequency) shifts ν effected by the channel in the sense that

$$\begin{aligned} y(t) &= \int_{\tau} \int_{\nu} S_{\mathbf{H}}^I(\tau, \nu) x(t - \tau) e^{j2\pi \nu t} d\tau d\nu \\ &= \int_{\tau} \int_{\nu} S_{\mathbf{H}}^O(\tau, \nu) x(t - \tau) e^{j2\pi \nu (t - \tau)} d\tau d\nu. \end{aligned} \quad (7)$$

Both $S_{\mathbf{H}}^I(\tau, \nu)$ and $S_{\mathbf{H}}^O(\tau, \nu)$ are special cases of the *generalized spreading function* [10] and related by a phase factor

$$S_{\mathbf{H}}^I(\tau, \nu) = S_{\mathbf{H}}^O(\tau, \nu) e^{-j2\pi \tau \nu}.$$

Because the magnitudes of $S_{\mathbf{H}}^I(\tau, \nu)$ and $S_{\mathbf{H}}^O(\tau, \nu)$ are equal, we shall hereafter use the shorthand notation $|S_{\mathbf{H}}(\tau, \nu)| \triangleq |S_{\mathbf{H}}^I(\tau, \nu)| = |S_{\mathbf{H}}^O(\tau, \nu)|$. Assuming the channel to be causal, there is $|S_{\mathbf{H}}(\tau, \nu)| = 0$ for $\tau \leq 0$.

We finally note that $L_{\mathbf{H}}^I(t, f)$ and $S_{\mathbf{H}}^I(\tau, \nu)$ as well as $L_{\mathbf{H}}^O(t, f)$ and $S_{\mathbf{H}}^O(\tau, \nu)$ are related by a 2-D (symplectic) Fourier transform [10].

B. Delay-Doppler Moments and Underspread Channels

It is common practice to distinguish between *underspread* and *overspread* channels (or targets, in a radar context), depending on the delays and Doppler shifts introduced by the channel [11]–[19]. Usually, this distinction is based on the assumption that the spreading function has compact support with maximum excess delay τ_{\max} and maximum Doppler frequency shift ν_{\max} , i.e., $|S_{\mathbf{H}}(\tau, \nu)| = 0$ for $(\tau, \nu) \notin [0, \tau_{\max}] \times [-\nu_{\max}, \nu_{\max}]$. The underspread property then means $\tau_{\max} \nu_{\max} \ll 1$ [11]–[19]. An alternative concept of underspread channels requires certain normalized moments of the spreading function to be small [12], [14], [15]. These moments are the *mean (excess) delays*³

$$\bar{\tau}_{\mathbf{H}}^{(1)} \triangleq \frac{1}{\|S_{\mathbf{H}}\|_1} \int_{\tau} \int_{\nu} |\tau - \tau_0| |S_{\mathbf{H}}(\tau, \nu)| d\tau d\nu \quad (8)$$

$$\bar{\tau}_{\mathbf{H}}^{(2)} \triangleq \frac{1}{\|S_{\mathbf{H}}\|_2} \sqrt{\int_{\tau} \int_{\nu} (\tau - \tau_0)^2 |S_{\mathbf{H}}(\tau, \nu)|^2 d\tau d\nu} \quad (9)$$

the *mean Doppler shifts*

$$\bar{\nu}_{\mathbf{H}}^{(1)} \triangleq \frac{1}{\|S_{\mathbf{H}}\|_1} \int_{\tau} \int_{\nu} |\nu| |S_{\mathbf{H}}(\tau, \nu)| d\tau d\nu \quad (10)$$

$$\bar{\nu}_{\mathbf{H}}^{(2)} \triangleq \frac{1}{\|S_{\mathbf{H}}\|_2} \sqrt{\int_{\tau} \int_{\nu} \nu^2 |S_{\mathbf{H}}(\tau, \nu)|^2 d\tau d\nu} \quad (11)$$

³Here, τ_0 is a suitable reference delay. Furthermore, the $L_p(\mathbb{R}^n)$ norm is defined as $\|f\|_p \triangleq [\int \dots \int |f(x_1, \dots, x_n)|^p dx_1 \dots dx_n]^{1/p}$ for $1 \leq p < \infty$ and $\|f\|_{\infty} \triangleq \sup |f(x_1, \dots, x_n)|$.

and the *mean delay-Doppler products*

$$\bar{\mu}_{\mathbf{H}}^{(1)} \triangleq \frac{1}{\|S_{\mathbf{H}}\|_1} \int_{\tau} \int_{\nu} |\tau - \tau_0| |\nu| |S_{\mathbf{H}}(\tau, \nu)| d\tau d\nu \quad (12)$$

$$\bar{\mu}_{\mathbf{H}}^{(2)} \triangleq \frac{1}{\|S_{\mathbf{H}}\|_2} \sqrt{\int_{\tau} \int_{\nu} (\tau - \tau_0)^2 \nu^2 |S_{\mathbf{H}}(\tau, \nu)|^2 d\tau d\nu}. \quad (13)$$

The underspread property then means that these moments (or specific products thereof) are $\ll 1$ [12], [14], [15].

The channel parameters in (8)–(13) will be used in Section V for the formulation of quantitative bounds on measurement errors. While their exact calculation would require perfect knowledge of the channel, in typical practical situations they can be coarsely determined by physical considerations (propagation environment, vehicle speed, etc.) or estimated from measurements (see Section VII-C).

III. CORRELATIVE CHANNEL SOUNDING METHODS

Whereas correlative sounding methods for mobile radio channels are usually described under the assumption of quasi-time-invariance [4]–[6], we here place them in a unifying mathematical framework for time-varying channels [7]. Most channel sounding methods are motivated by correlative identification techniques for time-invariant systems that are based on the following premises:

- In the noise-free⁴ case, a single measurement suffices since the channel does not change over time.
- Channel and receive filter commute, so that the “effective” sounding signal is determined by the series connection of transmit and receive filter (see Section III-B).

Unfortunately, for time-varying channels these assumptions do not hold, i.e., channel and receive filter do not commute and multiple measurements are required to track the channel variations. This results in systematic measurement errors that will be analyzed in Sections IV and V.

A. Idealized Impulse Channel Sounder

The simplest channel sounder [20] uses an impulse train with sounding period T as transmit signal

$$\Delta(t) \triangleq \sum_m \delta(t - mT)$$

so that the channel output is a superposition of “slices” of the kernel $k_{\mathbf{H}}(t, t')$ in (1),

$$y(t) = (\mathbf{H}\Delta)(t) = \int_{t'} k_{\mathbf{H}}(t, t') \Delta(t') dt' = \sum_m k_{\mathbf{H}}(t, mT). \quad (14)$$

This idealized channel sounder is a special case of the generic channel sounder model shown in Fig. 2, with transmit and receive filters $\mathbf{G} = \mathbf{R} = \mathbf{I}$ (the identity operator) so that $x(t) = \Delta(t)$ and $u(t) = y(t)$. If the maximum channel delay satisfies $\tau_{\max} \leq T$, then the m th block of the output signal $u(t)$ (the

⁴We consider a noise-free scenario since we are interested only in systematic measurement errors.

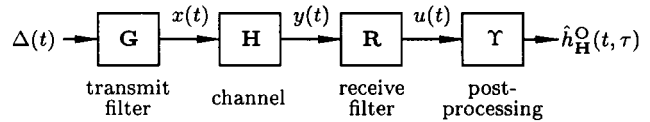


Fig. 2. Generic channel sounder (equivalent baseband model).

m th “channel snapshot”) can be shown [20] to equal the output delay spread function⁵ at time $t = mT$

$$u(\tau + mT) w(\tau) = h_{\mathbf{H}}^O(mT, \tau) \quad (15)$$

where $w(\tau) = 1$ for $0 < \tau < T$ and $w(\tau) = 0$ otherwise.

In practice, most sounder types record only every K th snapshot $h_{\mathbf{H}}^O(mKT, \tau)$, so that the *repetition period* of the measurements is $T_{\text{rep}} = KT$. If in addition to $\tau_{\max} \leq T$, the channel satisfies $\nu_{\max} \leq 1/(2KT) = 1/(2T_{\text{rep}})$, then the complete impulse response can be recovered without any error by interpolating between successive measurements [20],

$$\begin{aligned} h_{\mathbf{H}}^O(t, \tau) &= \sum_m h_{\mathbf{H}}^O(mT_{\text{rep}}, \tau) \text{sinc}\left(\frac{\pi}{T_{\text{rep}}}(t - mT_{\text{rep}})\right) \\ &= \sum_m u(\tau + mT_{\text{rep}}) w(\tau) \text{sinc}\left(\frac{\pi}{T_{\text{rep}}}(t - mT_{\text{rep}})\right) \end{aligned} \quad (16)$$

where $\text{sinc}(x) = \sin(x)/x$. For convenience, this transformation of $u(t)$ —alignment of the channel snapshots and interpolation—will be denoted by the operator Υ , i.e.,

$$(\Upsilon u)(t, \tau) \triangleq \sum_m u(\tau + mT_{\text{rep}}) w(\tau) \text{sinc}\left(\frac{\pi}{T_{\text{rep}}}(t - mT_{\text{rep}})\right). \quad (17)$$

Hence, (16) can be compactly written as (see Fig. 2)

$$h_{\mathbf{H}}^O(t, \tau) = (\Upsilon u)(t, \tau) = (\Upsilon \mathbf{H} \Delta)(t, \tau).$$

B. Generic Channel Sounder Model

While being conceptually simple, the idealized sounder is impractical since the impulse-train sounding signal $\Delta(t)$ has a prohibitively large (theoretically infinite) crest factor. It has thus become common to employ correlation/pulse-compression techniques. Fig. 2 shows a generic correlative channel sounder. The sounding signal is given by

$$x(t) = (\mathbf{G}\Delta)(t) = (g * \Delta)(t) = \sum_m g(t - mT) \quad (18)$$

where T is the sounding period, $g(t)$ is the impulse response of the linear, time-invariant (LTI) transmit filter \mathbf{G} , and $*$ denotes convolution. At the receiver, the channel output signal $y(t) = (\mathbf{H}x)(t)$ is passed through an LTI receive filter \mathbf{R} with impulse response $r(t)$, which results in the signal

$$u(t) = (r * y)(t) = (\mathbf{R}\mathbf{H}\mathbf{G}\Delta)(t).$$

Comparison with (14) shows that correlative channel sounding can also be viewed as idealized (i.e., impulse-train) sounding

⁵Note, however, that typically the channel sounder output is erroneously interpreted as $h_{\mathbf{H}}^1(t, \tau)$ (see Section IV).

of the composite channel **RHG**. Finally, estimates of the channel output delay spread function at $t = mT$, $\hat{h}_{\mathbf{H}}^{\mathbf{O}}(mT, \tau)$, are obtained from $u(t)$ according to (15). As mentioned above, most practical sounder types compute only every K th snapshot, which yields

$$\begin{aligned}\hat{h}_{\mathbf{H}}^{\mathbf{O}}(mT_{\text{rep}}, \tau) &= u(\tau + mT_{\text{rep}})w(\tau) \\ &= (\mathbf{RHG}\Delta)(\tau + mT_{\text{rep}})w(\tau).\end{aligned}$$

The final estimate is then obtained according to (17)

$$\hat{h}_{\mathbf{H}}^{\mathbf{O}}(t, \tau) = (\Upsilon u)(t, \tau) = (\Upsilon\mathbf{RHG}\Delta)(t, \tau). \quad (19)$$

If desired, an estimate of $L_{\mathbf{H}}^{\mathbf{O}}(mT_{\text{rep}}, f)$ [see (4)] can be obtained by Fourier transforming $\hat{h}_{\mathbf{H}}^{\mathbf{O}}(mT_{\text{rep}}, \tau)$,

$$\begin{aligned}\hat{L}_{\mathbf{H}}^{\mathbf{O}}(mT_{\text{rep}}, f) &= \int_{\tau} \hat{h}_{\mathbf{H}}^{\mathbf{O}}(mT_{\text{rep}}, \tau) e^{-j2\pi f\tau} d\tau \\ &= \int_{\tau} u(\tau + mT_{\text{rep}})w(\tau) e^{-j2\pi f\tau} d\tau.\end{aligned}$$

Hence, $\hat{L}_{\mathbf{H}}^{\mathbf{O}}(mT_{\text{rep}}, f)$ can be viewed as Fourier transform of the m th block of the received signal $u(t)$ or, alternatively, as short-time Fourier transform [21] of $u(t)$ using the analysis window $w(t)$, sampled at $t = mT_{\text{rep}}$. An estimate of $L_{\mathbf{H}}^{\mathbf{O}}(t, f)$ for arbitrary t can be obtained by interpolating $\hat{L}_{\mathbf{H}}^{\mathbf{O}}(mT_{\text{rep}}, f)$ or by Fourier transforming (with respect to τ) the interpolated impulse response $\hat{h}_{\mathbf{H}}^{\mathbf{O}}(t, \tau)$ in (19)

$$\hat{L}_{\mathbf{H}}^{\mathbf{O}}(t, f) = \int_{\tau} \hat{h}_{\mathbf{H}}^{\mathbf{O}}(t, \tau) e^{-j2\pi f\tau} d\tau. \quad (20)$$

We now consider the design of the transmit filter **G** [i.e., $g(t)$] and the receive filter **R** [i.e., $r(t)$]. If the channel is time-invariant, the receive filter **R** and the channel **H** commute, i.e., $\mathbf{RH} = \mathbf{HR}$, and thus we have

$$u(t) = (\mathbf{RHG}\Delta)(t) = (\mathbf{HRG}\Delta)(t) = (\mathbf{H}\tilde{\Delta})(t)$$

with the *virtual sounding signal*

$$\tilde{\Delta}(t) \triangleq (\mathbf{RG}\Delta)(t) = \sum_m (r * g)(t - mT). \quad (21)$$

Proper operation of the correlative channel sounder requires⁶ $(r * g)(t) \approx \delta(t)$, since then $\tilde{\Delta}(t) \approx \Delta(t)$. This means that the *effective* sounding signal is an impulse train whereas the actual sounding signal $x(t)$ [see (18)] can have a small crest factor. Note that this argument is based on the commutation of channel and receive filter and thus no longer holds for time-varying channels (see Section IV).

Subsequently, we discuss the three most common channel sounders within our general framework.

- *Correlation Sounder*. While all sounders considered here use correlation techniques, the term *correlation sounder* is usually reserved for sounders using a transmit pulse

$$g(t) = A \sum_{i=1}^N b_i c(t - iT_c) \quad (22)$$

⁶Note that it is actually sufficient to require $(r * g)(t) \approx B \sin c(\pi B(t - t_0))$ since only a bandlimited portion (with bandwidth B) of the channel is measured.

where $b_i \in \{-1, 1\}$ is a PN sequence and $c(t)$ is the (typically rectangular) chip pulse of length T_c . The length of $g(t)$ is thus $T_g = NT_c$. The receive filter is usually

$$r(t) = g(T_g - t) = A \sum_{i=1}^N b_{N-i+1} c(t - iT_c) \quad (23)$$

and thus has the same length $T_r = T_g = NT_c$. For N sufficiently large, the resulting virtual sounding signal $\tilde{\Delta}(t)$ in (21) approximates an impulse train over the bandwidth $1/(2T_c)$. Sounding sequences other than PN sequences and mismatched receive filters have also been proposed [22]–[26]; these variants still fit into our generic sounder model.

- *Swept Time-Delay Cross-Correlator (STDCC)*. Whereas the correlation sounder described above requires a sampling rate of $1/\Delta\tau$ to obtain a delay resolution of $\Delta\tau$, the STDCC allows to obtain the same resolution with a sampling rate of only $1/(K'\Delta\tau)$ where typically $K' \approx 5000$ [1], [27]. The price paid is a reduced channel tracking ability. In practical implementations, the receiver uses a dilated version of the transmitted PN sequence such that the receive filter is longer than the transmit filter by $\Delta\tau$, i.e., $T_r = T_g + \Delta\tau$. The repetition period is here defined as $T'_{\text{rep}} = K'T_r = 1/f_{\text{slip}}$ with the *slip rate* $f_{\text{slip}} = 1/T_g - 1/T_r = 1/T_g - 1/(T_g + \Delta\tau)$. The resulting estimate of the output delay spread function at time $t = mT'_{\text{rep}}$ and delay $\tau = k\Delta\tau$ is

$$\hat{h}_{\mathbf{H}}^{\mathbf{O}}(mT'_{\text{rep}}, k\Delta\tau) = u(mT'_{\text{rep}} + kT_r)w(k\Delta\tau).$$

Since $T'_{\text{rep}} \gg T_g$, the STDCC is significantly more sensitive to time variations of the channel than a conventional PN correlation sounder with small K .

- *Chirp Sounder*. Here, the transmit filter is given by

$$g(t) = A e^{j2\pi B((t^2/T_g) - t)}, \quad \text{for } 0 < t < T_g$$

and the receive filter equals $r(t) = g^*(T_g - t)$ [28]. The resulting virtual sounding signal $\tilde{\Delta}(t)$ in (21) approximates an impulse train within the band $[-B, B]$. Improved pulse-compression properties can be obtained by using nonrectangular (e.g., Gaussian) envelopes for $g(t)$ and $r(t)$ [29].

IV. MEASUREMENT ERRORS

For time-invariant channels, the sounding techniques described above are theoretically exact (assuming perfect pulse compression). However, for time-varying channels they are affected by systematic measurement errors that will be identified and analyzed in this section [7].

The overall measurement error $e(t, \tau)$ is given by the difference between the measurement $\hat{h}_{\mathbf{H}}^{\mathbf{O}}(t, \tau)$ in (19) and the desired true impulse response $h_{\mathbf{H}}^{\mathbf{I}}(t, \tau)$. We will now show that this error can be decomposed as

$$e(t, \tau) \triangleq \hat{h}_{\mathbf{H}}^{\mathbf{O}}(t, \tau) - h_{\mathbf{H}}^{\mathbf{I}}(t, \tau) = \sum_{i=1}^4 e_i(t, \tau) \quad (24)$$

with $e_1(t, \tau)$ being the *commutation error*, $e_2(t, \tau)$ the *pulse-compression error*, $e_3(t, \tau)$ the *aliasing error*, and $e_4(t, \tau)$ the *misinterpretation error*. These four error components will be defined and discussed in the following.

- 1) Recall that the actual ordering of transmit filter, channel, and receive filter is **RHG** whereas correlative sounding assumes the virtual ordering **HRG**, i.e., commutation of **H** and **R**. Unfortunately, a time-varying channel **H** does not commute with **R** and thus **RHG** \neq **HRG**, which causes the *commutation error*

$$\begin{aligned} e_1(t, \tau) &\triangleq \hat{h}_{\mathbf{H}}^{\mathbf{O}}(t, \tau) - (\mathbf{YHRG}\Delta)(t, \tau) \\ &= (\mathbf{YRH}x)(t, \tau) - (\mathbf{YHR}x)(t, \tau) \\ &= (\mathbf{Y}[\mathbf{R}, \mathbf{H}]x)(t, \tau). \end{aligned} \quad (25)$$

Here, the system $[\mathbf{R}, \mathbf{H}] \triangleq \mathbf{RH} - \mathbf{HR}$ is the *commutator* [30] of receive filter **R** and channel **H**. Note that $[\mathbf{R}, \mathbf{H}] = \mathbf{0}$ and thus $e_1(t, \tau) = 0$ only for an LTI channel **H**.

- 2) Imperfect pulse-compression properties of transmit and receive filter—i.e., $(r * g)(t) \neq \delta(t)$ or **RG** \neq **I**, and hence $\tilde{\Delta}(t) \neq \Delta(t)$ —lead to the *pulse-compression error*

$$\begin{aligned} e_2(t, \tau) &\triangleq (\mathbf{YHRG}\Delta)(t, \tau) - (\mathbf{YH}\Delta)(t, \tau) \quad (26) \\ &= (\mathbf{YH}\tilde{\Delta})(t, \tau) - (\mathbf{YH}\Delta)(t, \tau). \quad (27) \end{aligned}$$

This error also occurs in the time-invariant case. Usually, one attempts to reduce it via back-to-back calibration. However, for time-varying channels conventional calibration is also affected by systematic errors [7].

- 3) For channels with maximum delay $\tau_{\max} > T$, subsequent channel snapshots will overlap (aliasing in the delay domain). For channels with maximum Doppler shift $\nu_{\max} > 1/(2T_{\text{rep}})$, the channel variation is insufficiently tracked (aliasing in the Doppler domain). These two error mechanisms are combined in the *aliasing error*

$$e_3(t, \tau) \triangleq (\mathbf{YH}\Delta)(t, \tau) - h_{\mathbf{H}}^{\mathbf{O}}(t, \tau) \quad (28)$$

which is the deviation of the channel estimate obtained with the idealized channel sounder (i.e., perfect pulse compression), $\tilde{h}_{\mathbf{H}}^{\mathbf{O}}(t, \tau) \triangleq (\mathbf{YH}\Delta)(t, \tau)$, from the true output delay spread function $h_{\mathbf{H}}^{\mathbf{O}}(t, \tau)$.

Via the Fourier transform relation (6), an estimate of the channel's spreading function $S_{\mathbf{H}}^{\mathbf{O}}(\tau, \nu)$ can be obtained from $\tilde{h}_{\mathbf{H}}^{\mathbf{O}}(t, \tau)$ as⁷ (see Appendix C)

$$\begin{aligned} \tilde{S}_{\mathbf{H}}^{\mathbf{O}}(\tau, \nu) &\triangleq \int_{\tau} \tilde{h}_{\mathbf{H}}^{\mathbf{O}}(t, \tau) e^{-j2\pi f\tau} d\tau \\ &= I_{\mathcal{R}}(\tau, \nu) \sum_k \sum_l S_{\mathbf{H}}^{\mathbf{O}}\left(\tau + kT, \nu + \frac{l}{T_{\text{rep}}}\right) \\ &\quad \times e^{-j2\pi k(\nu + (l/T_{\text{rep}}))T} \end{aligned}$$

where $I_{\mathcal{R}}(\tau, \nu)$ is the indicator function of the delay-Doppler region $\mathcal{R} = [0, T] \times [-(1/2T_{\text{rep}}), (1/2T_{\text{rep}})]$

with $T_{\text{rep}} = KT$ [i.e., $I_{\mathcal{R}}(\tau, \nu)$ is 1 for $(\tau, \nu) \in \mathcal{R}$ and 0 elsewhere]. For channels with maximum delay τ_{\max} and maximum Doppler shift ν_{\max} such that

$$\tau_{\max} \leq T \leq \frac{1}{2K\nu_{\max}} \quad (29)$$

we have $\tilde{S}_{\mathbf{H}}^{\mathbf{O}}(\tau, \nu) = S_{\mathbf{H}}^{\mathbf{O}}(\tau, \nu)$ and thus $\tilde{h}_{\mathbf{H}}^{\mathbf{O}}(t, \tau) = h_{\mathbf{H}}^{\mathbf{O}}(t, \tau)$, i.e., $e_3(t, \tau) \equiv 0$ (this result was previously derived in [20]). Note that the condition (29) for perfect identification requires $\tau_{\max}\nu_{\max} \leq 1/(2K)$, i.e., an *underspread* channel as defined in Section II-B.

- 4) Finally, the measured function $\hat{h}_{\mathbf{H}}^{\mathbf{O}}(t, \tau)$ is typically used as an estimate of the impulse response $h_{\mathbf{H}}^{\mathbf{I}}(t, \tau)$ whereas according to Subsection III-A it is rather an estimate of the output delay spread function $h_{\mathbf{H}}^{\mathbf{O}}(t, \tau)$. This corresponds to the *misinterpretation error*

$$e_4(t, \tau) \triangleq h_{\mathbf{H}}^{\mathbf{O}}(t, \tau) - h_{\mathbf{H}}^{\mathbf{I}}(t, \tau). \quad (30)$$

Misinterpretation can easily be avoided by correctly interpreting the measurement as an estimate of $h_{\mathbf{H}}^{\mathbf{O}}(t, \tau)$ or via the conversion $\hat{h}_{\mathbf{H}}^{\mathbf{I}}(t, \tau) = \hat{h}_{\mathbf{H}}^{\mathbf{O}}(t - \tau, \tau)$ [see (2)].

It is readily checked that the sum of the four error components $e_i(t, \tau)$ is indeed equal to the total measurement error $e(t, \tau) = \hat{h}_{\mathbf{H}}^{\mathbf{O}}(t, \tau) - h_{\mathbf{H}}^{\mathbf{I}}(t, \tau)$, as was stated in (24).

In a similar way, the difference between the measured function $\hat{L}_{\mathbf{H}}^{\mathbf{O}}(t, f)$ in (20) and the desired time-varying transfer function $L_{\mathbf{H}}^{\mathbf{I}}(t, f)$ can be written as

$$L_e(t, f) \triangleq \hat{L}_{\mathbf{H}}^{\mathbf{O}}(t, f) - L_{\mathbf{H}}^{\mathbf{I}}(t, f) = \sum_{i=1}^4 L_{e_i}(t, f) \quad (31)$$

with $L_{e_i}(t, f) \triangleq \mathcal{F}_{\tau \rightarrow f}\{e_i(t, \tau)\}$ being a time-frequency representation of the error component $e_i(t, \tau)$.

V. ERROR BOUNDS

Next, we present a quantitative analysis of the error components $e_i(t, \tau)$ and $L_{e_i}(t, f)$ via upper bounds on specific error norms [7]. These bounds are formulated in terms of important channel and sounder parameters. We note that for arbitrary norms $\|\cdot\|$, application of the triangle inequality to (24) and (31) gives

$$\|e\| \leq \sum_{i=1}^4 \|e_i\| \quad \text{and} \quad \|L_e\| \leq \sum_{i=1}^4 \|L_{e_i}\|$$

respectively. Thus, our upper bounds on the error components $e_i(t, \tau)$ and $L_{e_i}(t, f)$ also yield upper bounds on the total errors $e(t, \tau) = \hat{h}_{\mathbf{H}}^{\mathbf{O}}(t, \tau) - h_{\mathbf{H}}^{\mathbf{I}}(t, \tau)$ and $L_e(t, f) = \hat{L}_{\mathbf{H}}^{\mathbf{O}}(t, f) - L_{\mathbf{H}}^{\mathbf{I}}(t, f)$, respectively. Furthermore, due to the Fourier transform relating $e_i(t, \tau)$ and $L_{e_i}(t, f)$, there is

$$|L_{e_i}(t, f)| = \left| \int_{\tau} e_i(t, \tau) e^{-j2\pi f\tau} d\tau \right| \leq \int_{\tau} |e_i(t, \tau)| d\tau \quad (32)$$

$$\|L_{e_i}\|_2 = \|e_i\|_2. \quad (33)$$

⁷A similar result was obtained in a speech analysis context in [31].

A. Commutation Error Bounds

We first consider the commutation error $e_1(t, \tau) = (\Upsilon[\mathbf{R}, \mathbf{H}]x)(t, \tau)$ in (25). Whereas $[\mathbf{R}, \mathbf{H}]$ is generally nonzero for an LTV channel \mathbf{H} , it was shown in [12], [13] that for \mathbf{R}, \mathbf{H} jointly underspread [12], [13] there is $[\mathbf{R}, \mathbf{H}] \approx \mathbf{0}$, which entails $e_1(t, \tau) \approx 0$. Indeed, we show in Appendix A that for⁸ $T_g \leq T$ the magnitude of the commutation error $e_1(t, \tau)$ at $t = mT_{\text{rep}}$ is upper bounded as⁹

$$\frac{|e_1(mT_{\text{rep}}, \tau)|}{\|g\|_\infty \|\mathbf{S}_{\mathbf{H}}\|_1 \|r\|_1} \leq \varepsilon_1^{(1)} \triangleq 2\pi \bar{\tau}_{\mathbf{R}}^{(1)} \bar{\nu}_{\mathbf{H}}^{(1)} \quad (34)$$

where

$$\bar{\tau}_{\mathbf{R}}^{(1)} \triangleq \frac{1}{\|r\|_1} \int_{\tau} |r(\tau)| d\tau \quad (35)$$

is the mean duration of the receive filter $r(t)$ and $\bar{\nu}_{\mathbf{H}}^{(1)}$ is the channel's mean Doppler shift as defined in (10).

Since the postprocessing operator Υ incorporates the window $w(\tau)$ [see (17)], it follows that $e_1(t, \tau) = (\Upsilon[\mathbf{R}, \mathbf{H}]x)(t, \tau)$ is nonzero only for $0 \leq \tau \leq T$ and hence

$$\begin{aligned} \int_{\tau} |e_1(mT_{\text{rep}}, \tau)|^p d\tau &= \int_0^T |e_1(mT_{\text{rep}}, \tau)|^p d\tau \\ &\leq \max_{\tau} |e_1(mT_{\text{rep}}, \tau)|^p \int_0^T d\tau \\ &= T \max_{\tau} |e_1(mT_{\text{rep}}, \tau)|^p \end{aligned}$$

for arbitrary p . Together with (34), this yields the bounds

$$\frac{\int_{\tau} |e_1(mT_{\text{rep}}, \tau)| d\tau}{\|g\|_\infty \|\mathbf{S}_{\mathbf{H}}\|_1 \|r\|_1} \leq T \varepsilon_1^{(1)} \quad (36)$$

$$\frac{\sqrt{\int_{\tau} |e_1(mT_{\text{rep}}, \tau)|^2 d\tau}}{\|g\|_\infty \|\mathbf{S}_{\mathbf{H}}\|_1 \|r\|_1} \leq \sqrt{T} \varepsilon_1^{(1)}. \quad (37)$$

For typical receive filters that have constant envelope within the interval $[0, T_r]$ and are zero otherwise, $\bar{\tau}_{\mathbf{R}}^{(1)} = T_r/2$. Hence, the above bounds imply that if the product of the channel's mean Doppler shift $\bar{\nu}_{\mathbf{H}}^{(1)}$ and the receive filter's duration T_r is small, the commutation error $e_1(mT_{\text{rep}}, \tau)$ will be small too. We note that the requirement of small T_r conflicts with the desire to use large filter lengths in order to obtain better pulse-compression properties (see Sections V-B and VI-A).

In order to obtain further bounds, we assume that $(\Upsilon\mathbf{R}\mathbf{H}\mathbf{G}\Delta)(t, \tau) = h_{\mathbf{RHG}}^{\mathbf{O}}(t, \tau)$ and $(\Upsilon\mathbf{H}\mathbf{R}\mathbf{G}\Delta)(t, \tau) = h_{\mathbf{HRG}}^{\mathbf{O}}(t, \tau)$, which means that the idealized measurements of the composite channels \mathbf{RHG} and \mathbf{HRG} feature no aliasing errors. With this assumption, one can show that

$$\frac{\int_{\tau} |e_1(t, \tau)| d\tau}{\|g\|_1 \|\mathbf{S}_{\mathbf{H}}\|_1 \|r\|_1} \leq \varepsilon_1^{(1)} \quad (38)$$

⁸The assumption $T_g \leq T$ means that subsequent transmit pulses do not overlap. If this is not the case, the bound remains valid if $\|g\|_\infty$ is replaced by $\|x\|_\infty$.

⁹Note that this can be equivalently formulated as an upper bound on $\|e_1(mT_{\text{rep}}, \cdot)\|_\infty = \sup_{\tau} |e_1(mT_{\text{rep}}, \tau)|$ since (34) is valid for all τ . A similar remark applies to several subsequent bounds.

$$\frac{\|e_1\|_2}{\|g\|_1 \|\mathbf{S}_{\mathbf{H}}\|_2 \|r\|_1} \leq \varepsilon_1^{(2)} \triangleq 2\pi \left[\bar{\mu}_{\mathbf{RH}}^{(2)} + \bar{\mu}_{\mathbf{H}}^{(2)} \right] \quad (39)$$

with $\bar{\mu}^{(2)}$ as defined in (13). A proof of the first bound is provided in Appendix A. Using (32) and (33), it further follows that these bounds also apply to the L_∞ and L_2 norms of $L_{e_1}(t, f) = \hat{L}_{\mathbf{H}}^{\mathbf{O}}(t, f) - L_{\mathbf{HRG}}^{\mathbf{O}}(t, f)$, i.e.,

$$\frac{|L_{e_1}(t, f)|}{\|g\|_1 \|\mathbf{S}_{\mathbf{H}}\|_1 \|r\|_1} \leq \varepsilon_1^{(1)}, \quad \frac{\|L_{e_1}\|_2}{\|g\|_1 \|\mathbf{S}_{\mathbf{H}}\|_2 \|r\|_1} \leq \varepsilon_1^{(2)}.$$

B. Pulse-Compression Error Bounds

Next, we consider the pulse-compression error $e_2(t, \tau) = (\Upsilon\mathbf{H}\tilde{\Delta})(t, \tau) - (\Upsilon\mathbf{H}\Delta)(t, \tau)$ as defined in (27). As noted previously, the transmit and receive filters are required to yield good pulse compression, i.e., $R(f)G(f) \approx 1$, only within the measurement band $[-B, B]$. This is reflected by the following error bounds. In particular, it is shown in Appendix B that the magnitude of $e_2(t, \tau)$ at $t = mT_{\text{rep}}$ is upper bounded as

$$\frac{|e_2(mT_{\text{rep}}, \tau)|}{\|\mathbf{S}_{\mathbf{H}}\|_1} \leq \varepsilon_2 \triangleq \frac{1}{T} \sum_{|k| \leq BT} \left| R\left(\frac{k}{T}\right) G\left(\frac{k}{T}\right) - 1 \right| \quad (40)$$

where $R(f)$ and $G(f)$ are the Fourier transforms of $r(t)$ and $g(t)$, respectively. This further induces the bounds

$$\frac{\int_{\tau} |e_2(mT_{\text{rep}}, \tau)| d\tau}{\|\mathbf{S}_{\mathbf{H}}\|_1} \leq T \varepsilon_2 \quad (41)$$

$$\frac{\sqrt{\int_{\tau} |e_2(mT_{\text{rep}}, \tau)|^2 d\tau}}{\|\mathbf{S}_{\mathbf{H}}\|_1} \leq \sqrt{T} \varepsilon_2. \quad (42)$$

According to (40), these bounds are determined by the deviation of the composite transfer function of transmit filter and receive filter, $R(f)G(f)$, from the ideal value 1 (within the measurement band $[-B, B]$).

For the following bounds, we assume that $(\Upsilon\mathbf{H}\Delta)(t, \tau) = h_{\mathbf{H}}^{\mathbf{O}}(t, \tau)$ and $(\Upsilon\mathbf{H}\mathbf{R}\mathbf{G}\Delta)(t, \tau) = h_{\mathbf{HRG}}^{\mathbf{O}}(t, \tau)$, i.e., that no aliasing errors are present in the idealized measurements of \mathbf{H} and \mathbf{HRG} . It is then shown in Appendix B that

$$\frac{\int_{\tau} |e_2(t, \tau)| d\tau}{\|\mathbf{S}_{\mathbf{H}}\|_1} \leq d_1 \triangleq \int_{\tau} |(r * g * \text{sinc}_B)(\tau) - \text{sinc}_B(\tau)| d\tau \quad (43)$$

$$\frac{|L_{e_2}(t, f)|}{\|\mathbf{S}_{\mathbf{H}}\|_1} \leq d_1 \quad (44)$$

where $\text{sinc}_B(\tau) \triangleq B \text{sinc}(\pi B\tau)$, and

$$\frac{\|e_2\|_2}{\|\mathbf{S}_{\mathbf{H}}\|_2} \leq D_\infty \triangleq \max_{f \in [-B, B]} |R(f)G(f) - 1| \quad (45)$$

$$\frac{\|L_{e_2}\|_2}{\|\mathbf{S}_{\mathbf{H}}\|_2} \leq D_\infty. \quad (46)$$

For typical correlation or chirp sounders, these error bounds will decrease with increasing transmit/receive filter length. The above error bounds (just as the pulse-compression error itself) do not depend on the channel and are valid for time-varying and time-invariant channels.

C. Aliasing Error Bounds

The aliasing error $e_3(t, \tau) = (\Upsilon\mathbf{H}\Delta)(t, \tau) - h_{\mathbf{H}}^{\mathbf{O}}(t, \tau)$ in (28) will be nonzero unless the condition (29) for perfect identification is met. In Appendix C, the following bounds¹⁰ on the aliasing error are derived:

$$\frac{\int_{\tau} |e_3(t, \tau)| d\tau}{\|\mathbf{S}_{\mathbf{H}}\|_1} \leq \varepsilon_3^{(1)} \triangleq 2 \left[\frac{\bar{\tau}_{\mathbf{H}}^{(1)}}{T - \tau_0} + 2KT\bar{\nu}_{\mathbf{H}}^{(1)} \right] \quad (47)$$

$$\frac{\|e_3\|_2}{\|\mathbf{S}_{\mathbf{H}}\|_2} \leq \varepsilon_3^{(2)} \triangleq 2 \left[\left(\frac{\bar{\tau}_{\mathbf{H}}^{(2)}}{T - \tau_0} \right)^2 + \left(2KT\bar{\nu}_{\mathbf{H}}^{(2)} \right)^2 \right]^{1/2}. \quad (48)$$

Here, $\bar{\tau}_{\mathbf{H}}^{(1)}$, $\bar{\tau}_{\mathbf{H}}^{(2)}$ and $\bar{\nu}_{\mathbf{H}}^{(1)}$, $\bar{\nu}_{\mathbf{H}}^{(2)}$ are the mean delay and Doppler shift parameters in (8)–(11), and it is assumed that $T > \tau_0$ [recall that τ_0 is the reference delay occurring in the definition of $\bar{\tau}_{\mathbf{H}}^{(1)}$ and $\bar{\tau}_{\mathbf{H}}^{(2)}$, see (8), (9)]. Furthermore, it follows with (32) and (33) that the corresponding transfer function error $L_{e_3}(t, f)$ is bounded as

$$\frac{|L_{e_3}(t, f)|}{\|\mathbf{S}_{\mathbf{H}}\|_1} \leq \varepsilon_3^{(1)}, \quad \frac{\|L_{e_3}\|_2}{\|\mathbf{S}_{\mathbf{H}}\|_2} \leq \varepsilon_3^{(2)}.$$

In the error bounds $\varepsilon_3^{(i)}$, the term $\bar{\tau}_{\mathbf{H}}^{(i)}/(T - \tau_0)$ corresponds to aliasing with respect to τ (i.e., overlapping snapshots) and the term $2KT\bar{\nu}_{\mathbf{H}}^{(i)}$ corresponds to aliasing with respect to ν (i.e., insufficient channel tracking). The values of K and T in relation to $\bar{\tau}_{\mathbf{H}}^{(i)}$ and $\bar{\nu}_{\mathbf{H}}^{(i)}$ determine which aliasing type dominates the bounds. A balanced choice of T that minimizes $\varepsilon_3^{(i)}$ will be described in Section VI-B.

The above bounds are convenient in that they depend only on $\bar{\tau}_{\mathbf{H}}^{(i)}$ and $\bar{\nu}_{\mathbf{H}}^{(i)}$ and thus do not require a more detailed characterization of the channel. On the other hand, for the same reason they tend to be rather loose.

D. Misinterpretation Error Bounds

Finally, we consider the misinterpretation error $e_4(t, \tau) = h_{\mathbf{H}}^{\mathbf{O}}(t, \tau) - h_{\mathbf{H}}^{\mathbf{I}}(t, \tau)$ as defined in (30). In [12] it was shown that the corresponding transfer function difference $L_{e_4}(t, f) = L_{\mathbf{H}}^{\mathbf{O}}(t, f) - L_{\mathbf{H}}^{\mathbf{I}}(t, f)$ is bounded as

$$\frac{|L_{e_4}(t, f)|}{\|\mathbf{S}_{\mathbf{H}}\|_1} \leq \varepsilon_4^{(1)} \triangleq 2\pi\bar{\mu}_{\mathbf{H}}^{(1)}, \quad \frac{\|L_{e_4}\|_2}{\|\mathbf{S}_{\mathbf{H}}\|_2} \leq \varepsilon_4^{(2)} \triangleq 2\pi\bar{\mu}_{\mathbf{H}}^{(2)}.$$

It can be shown similarly that $e_4(t, \tau)$ is bounded as

$$\frac{\int_{\tau} |e_4(t, \tau)| d\tau}{\|\mathbf{S}_{\mathbf{H}}\|_1} \leq \varepsilon_4^{(1)}, \quad \frac{\|e_4\|_2}{\|\mathbf{S}_{\mathbf{H}}\|_2} \leq \varepsilon_4^{(2)} \quad (49)$$

[the second bound follows with (33)]. These bounds involve the channel's mean delay-Doppler products $\bar{\mu}_{\mathbf{H}}^{(i)}$ as defined in (12) and (13); these will be small for underspread channels. Of course, the bounds do not depend on any sounding parameters or on the sounding method itself. As was mentioned in Section IV, the effect of misinterpretation can easily be avoided

¹⁰These bounds do not apply directly to STDCC sounders. However, slight modifications of the proof in Appendix C yield qualitatively similar bounds for the STDCC.

by converting the estimate $\hat{h}_{\mathbf{H}}^{\mathbf{O}}(t, \tau)$ according to $\hat{h}_{\mathbf{H}}^{\mathbf{I}}(t, \tau) = \hat{h}_{\mathbf{H}}^{\mathbf{O}}(t - \tau, \tau)$.

VI. CHOICE OF SOUNDER PARAMETERS

Based on the above error bounds, we next present guidelines for the choice of two important sounder parameters: transmit/receive filter length and sounding period.

A. Choice of the Filter Length

We first consider the filter length $T_r = T_g$ (note that the transmit and receive filter lengths are assumed equal). In Sections V-A and V-B, it was shown that the commutation error increases with increasing filter length whereas the pulse-compression error usually decreases with increasing filter length. Thus, the choice of the filter length corresponds to a tradeoff between small commutation error and small pulse-compression error.

In what follows, we will calculate the filter length that minimizes an upper bound on the sum of commutation error and pulse-compression error. For simplicity, we restrict our attention to correlation sounders, i.e., sounders using PN sequences [see (22) and (23)]. Furthermore, we assume that the sounding period equals the filter length, $T = T_r = T_g$. The chip length T_c corresponding to a fixed measurement bandwidth B equals $T_c = 1/(2B)$. The filter length $T_r = T_g$ then corresponds to the PN sequence length N via $T_r = NT_c$ and (35) gives $\bar{\tau}_{\mathbf{R}}^{(1)} = T_r/2 = NT_c/2 = N/(4B)$. The transmit and receive filters are normalized so that $A = 1/\sqrt{T}$ in (22) and hence $\|g\|_{\infty} = 1/\sqrt{T}$ and $\|r\|_1 = \sqrt{T}$. Inserting these values into (34) yields $|e_1(mT_{\text{rep}}, \tau)|/\|\mathbf{S}_{\mathbf{H}}\|_1 \leq N(\pi\bar{\nu}_{\mathbf{H}}^{(1)})/(2B)$. Furthermore, it can be shown that (40) can further be bounded as $|e_2(mT_{\text{rep}}, \tau)|/\|\mathbf{S}_{\mathbf{H}}\|_1 \leq 2/N$. The sum of commutation error and pulse-compression error, $e_1(mT_{\text{rep}}, \tau) + e_2(mT_{\text{rep}}, \tau)$, is thus bounded as

$$\begin{aligned} & \frac{|e_1(mT_{\text{rep}}, \tau) + e_2(mT_{\text{rep}}, \tau)|}{\|\mathbf{S}_{\mathbf{H}}\|_1} \\ & \leq \frac{|e_1(mT_{\text{rep}}, \tau)|}{\|\mathbf{S}_{\mathbf{H}}\|_1} + \frac{|e_2(mT_{\text{rep}}, \tau)|}{\|\mathbf{S}_{\mathbf{H}}\|_1} \\ & \leq N \frac{\pi\bar{\nu}_{\mathbf{H}}^{(1)}}{2B} + \frac{2}{N}. \end{aligned} \quad (50)$$

This bound is minimized by

$$N = \sqrt{\frac{4B}{\pi\bar{\nu}_{\mathbf{H}}^{(1)}}}$$

which corresponds to an optimal balance between the bounds on the error components $e_1(t, \tau)$ and $e_2(t, \tau)$. The resulting minimum upper bound in (50) equals $2\sqrt{\pi\bar{\nu}_{\mathbf{H}}^{(1)}/B}$. Since in practice $N = 2^l - 1$ with some l , our final design rule is to choose the PN sequence length according to

$$N_{\text{opt}} = 2^{l_{\text{opt}}} - 1 \quad \text{with } l_{\text{opt}} = \text{round} \left\{ \log_2 \left(\sqrt{\frac{4B}{\pi\bar{\nu}_{\mathbf{H}}^{(1)}}} + 1 \right) \right\}. \quad (51)$$

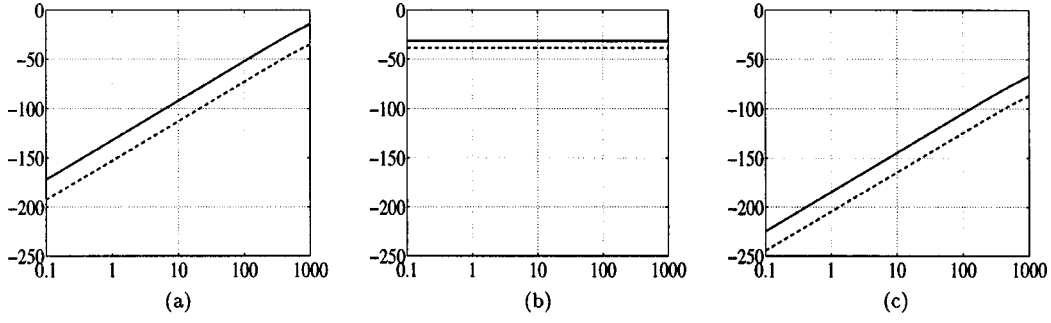


Fig. 3. Systematic measurement errors (dashed line) and corresponding upper bounds (solid line), both in decibels, for a synthetic two-path channel. (a) Maximum integrated commutation error. (b) Maximum integrated pulse-compression error. (c) Maximum integrated misinterpretation error. (In this example, there was no aliasing error.) The horizontal axis is the channel's Doppler shift ν_{\max} in hertz.

B. Choice of the Sounding Period

According to Section V-C, the sounding period T and the repetition factor K are the sounder parameters that determine the aliasing error. Using (47) and (48) with $\tau_0 = 0$ (similar results exist for arbitrary τ_0 but are more difficult to interpret), it follows that the bounds $\varepsilon_3^{(1)}$ and $\varepsilon_3^{(2)}$ on the aliasing error are minimized (for fixed K) by choosing the sounding period as

$$T_{\text{opt}}^{(i)} = \sqrt{\frac{\bar{\tau}_{\mathbf{H}}^{(i)}}{2K\bar{\nu}_{\mathbf{H}}^{(i)}}}, \quad i = 1, 2. \quad (52)$$

The resulting minimum value of $\varepsilon_3^{(i)}$ is

$$\varepsilon_{3,\min}^{(i)} = 4\sqrt{2K\bar{\tau}_{\mathbf{H}}^{(i)}\bar{\nu}_{\mathbf{H}}^{(i)}}, \quad i = 1, 2. \quad (53)$$

For an interpretation, we recall from Section V-C that the aliasing error is caused by aliasing in the delay variable and aliasing in the Doppler variable. The sounding periods $T_{\text{opt}}^{(i)}$ achieve an optimal balance between the terms $\bar{\tau}_{\mathbf{H}}^{(i)}/T$ and $2KT\bar{\nu}_{\mathbf{H}}^{(i)}$ in the bounds (47), (48) that are associated to these two aliasing mechanisms. Furthermore, (53) shows that $\varepsilon_{3,\min}^{(i)}$ is determined by the product of $\bar{\tau}_{\mathbf{H}}^{(i)}$ and $\bar{\nu}_{\mathbf{H}}^{(i)}$; it will thus be small if the channel is underspread. Of course, in practice other criteria not considered in our optimization (like computational or storage requirements) may suggest to use sounding periods different from $T_{\text{opt}}^{(1)}$ or $T_{\text{opt}}^{(2)}$.

VII. SIMULATION AND MEASUREMENT RESULTS

We next present computer experiments illustrating our theoretical results, and we demonstrate how our results can be used to assess the accuracy of measured data.

A. Measurement Errors for a Simulated Channel

In our first experiment, we simulated the sounding of a synthetic two-path channel with carrier frequency 1.8 GHz. The baseband channel's impulse response is

$$h_{\mathbf{H}}^{\text{I}}(t, \tau) = a_0 \delta(\tau) + a_1 \cos(2\pi\nu_{\max}t) \delta(\tau - \tau_{\max}). \quad (54)$$

This channel consists of a direct path with constant amplitude $a_0 = 1$ and a second path with delay $\tau_{\max} = 2\mu\text{s}$ and sinusoidally varying amplitude with peak amplitude $a_1 = 0.4$. The Doppler shift ν_{\max} was varied between 0.1 and 1000 Hz, corre-

sponding to a velocity ranging from 0.06 to 600 km/h. We assumed a correlation sounder using a PN sequence of length $N = 127$ and repetition factor $K = 1$. With the sampling frequency (double measurement bandwidth B) assumed as 10 MHz, the duration of the PN sequence (=filter length = sounding period) is $T_g = T_r = T = 12 \cdot 7\mu\text{s}$.

In this example, the aliasing error is zero since with $\tau_{\max} = 2\mu\text{s}$, $\nu_{\max} \leq 1000$ Hz, $T = 12 \cdot 7\mu\text{s}$, and $K = 1$ condition (29) is satisfied. The other three error components and their upper bounds are compared for various values of ν_{\max} in Fig. 3. The short PN sequence caused the pulse-compression error to dominate. The maximum integrated pulse-compression error $\max_m \{(1/T) \int_{\tau} |e_2(mT, \tau)| d\tau\}$ and the corresponding upper bound $\|S_{\mathbf{H}}\|_1 \varepsilon_2$ according to (41) were calculated as $5.9 \cdot 10^{-3}$ and $7.8 \cdot 10^{-3}$, respectively, independently of ν_{\max} [see Fig. 3(b)]. The maximum integrated commutation error $\max_m \{(1/T) \int_{\tau} |e_1(mT, \tau)| d\tau\}$ and the corresponding upper bound $\|g\|_{\infty} \|S_{\mathbf{H}}\|_1 \|r\|_1 \varepsilon_1^{(1)}$ according to (36) are shown in Fig. 3(a) as a function of ν_{\max} . Similarly, the maximum integrated misinterpretation error $\max_m \{(1/T) \int_{\tau} |e_4(mT, \tau)| d\tau\}$ and the corresponding upper bound $2\pi \|S_{\mathbf{H}}\|_1 \bar{\nu}_{\mathbf{H}}^{(1)}/T$ according to (49) are shown in Fig. 3(c). It is seen that the commutation and misinterpretation errors and the corresponding upper bounds grow with increasing ν_{\max} ; however, in this example the misinterpretation error always stays well below the commutation and pulse-compression errors.

The total error $\max_m \{(1/T) \int_{\tau} |\hat{h}_{\mathbf{H}}^{\text{O}}(mT, \tau) - h_{\mathbf{H}}^{\text{I}}(mT, \tau)| d\tau\}$ and the associated bound are shown in Fig. 4(a). Comparing with Fig. 3, we see that whereas up to about $\nu_{\max} = 200$ Hz the (constant) pulse-compression error dominates, for $\nu_{\max} > 200$ Hz the commutation error dominates. For comparison, Fig. 4(b) shows the total error and corresponding bound when the same two-path channel is sounded with a PN sequence of length $N = 1023$. It is seen that the value of ν_{\max} where the commutation error starts to dominate has dropped to about 50 Hz. This confirms our result [see (51)] that for different maximum Doppler shifts ν_{\max} different values of N are preferable. The choice of N for a given ν_{\max} is considered in the next subsection.

B. Choice of Filter Length for the Simulated Channel

Our next experiment investigates the influence of the transmit/receive filter length (equivalently, PN sequence

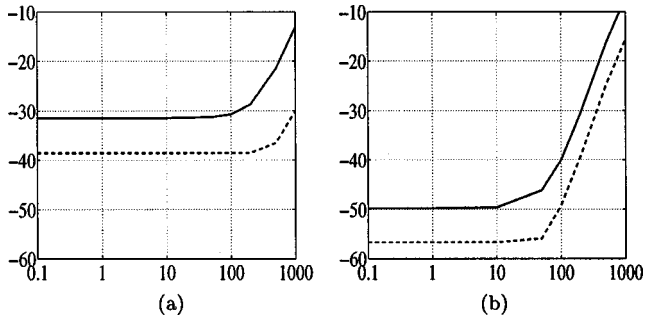


Fig. 4. Total systematic measurement error (dashed line) and corresponding upper bound (solid line) in dB for the synthetic two-path channel. (a) PN sequence length $N = 127$. (b) PN sequence length $N = 1023$. The horizontal axis is the channel's Doppler shift ν_{\max} in Hz.

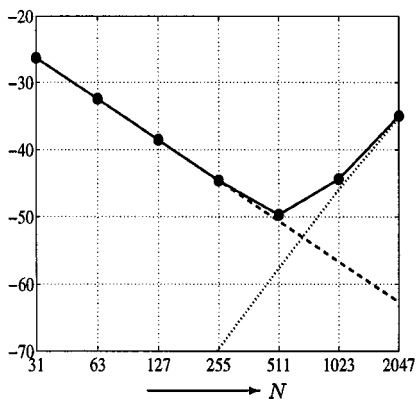


Fig. 5. Maximum magnitude (in dB) of the commutation error (dotted line), of the pulse-compression error (dashed line), and of their sum (solid line) as a function of the PN sequence length N for the synthetic two-path channel with $\nu_{\max} = 60$ Hz.

length) on the measurement accuracy, and illustrates the fact that a good choice of the PN sequence length balances commutation error and pulse-compression error. We sounded the same two-path channel as in the previous section, with $\nu_{\max} = 60$ Hz, using PN sequences of length $N = 2^l - 1$ with $l = 5, \dots, 11$. Fig. 5 shows the maximum magnitude of the commutation error, $\max_{m, \tau} |e_1(mT, \tau)|$, of the pulse-compression error, $\max_{m, \tau} |e_2(mT, \tau)|$, and of their sum, $\max_{m, \tau} |e_1(mT, \tau) + e_2(mT, \tau)|$, as a function of N . It is seen that these errors are best balanced for $N = 511$ since $\max_{m, \tau} |e_1(mT, \tau) + e_2(mT, \tau)|$ features a pronounced minimum at this point. This agrees with our theoretical guideline (51) which also yields $N_{\text{opt}} = 2^{l_{\text{opt}}} - 1 = 511$.

Table I contrasts the PN sequence length according to (51), $N_{\text{opt}} = 2^{l_{\text{opt}}} - 1$, with the truly optimum PN sequence length (hereafter denoted N_{min}) for a variety of Doppler frequencies. Note that N_{min} minimizes the actual sum of commutation error and pulse-compression error whereas N_{opt} minimizes just the corresponding upper bound (see the analysis in Section VI-A). Furthermore, whereas calculation of $N_{\text{opt}} = 2^{l_{\text{opt}}} - 1$ according to (51) only requires knowledge of $\hat{\nu}_{\mathbf{H}}^{(1)}$, calculation of N_{min} requires complete knowledge of the channel's impulse response. Nevertheless, it is seen that our guideline N_{opt} almost always agrees with N_{min} .

TABLE I
TRULY OPTIMAL PN SEQUENCE LENGTH N_{min} AND PN SEQUENCE LENGTH N_{opt} ACCORDING TO (51) FOR THE SYNTHETIC TWO-PATH CHANNEL WITH VARIOUS DOPPLER SHIFTS ν_{\max}

ν_{\max} / Hz	10	30	50	100	300	500	1000
$\hat{\nu}_{\mathbf{H}}^{(1)} / \text{Hz}$	2.9	8.6	14.3	28.6	85.7	142.9	285.7
N_{min}	2047	1023	1023	511	255	127	127
N_{opt}	2047	1023	511	511	255	255	127

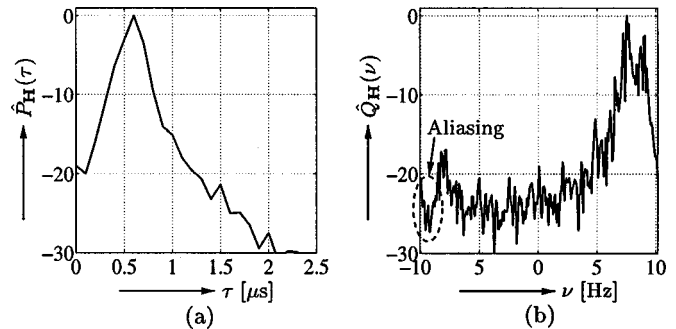


Fig. 6. (a) Estimated delay profile $\hat{P}_{\mathbf{H}}(\tau)$ and (b) estimated Doppler profile $\hat{Q}_{\mathbf{H}}(\nu)$ (both in dB) obtained from measurements of a typical suburban mobile radio channel.

C. Evaluation of Measurements

In order to demonstrate the use of our error bounds for assessing the accuracy of existing measurements, we analyzed measurement results obtained with a RUSK XL channel sounder [25]. The carrier frequency was 1.8 GHz. The receiver part of the sounder was located in a vehicle that moved with average velocity 5.9 km/h (corresponding to a Doppler shift of 9.83 Hz) through a typical suburban environment. The sampling frequency (double measurement bandwidth B) was 10 MHz, corresponding to a delay resolution of $0.1 \mu\text{s}$. Each impulse response snapshot consisted of 1024 samples (corresponding to sounding period $T = 102.4 \mu\text{s}$), which was also the length of the transmit and receive filters. The repetition factor was $K = 480$ so that $T_{\text{rep}} = 49.152$ ms.

The measured data were used to compute an estimate $\hat{S}_{\mathbf{H}}(\tau, \nu)$ of the channel's spreading function, an estimated delay profile $\hat{P}_{\mathbf{H}}(\tau) = \int_{\nu} |\hat{S}_{\mathbf{H}}(\tau, \nu)| d\nu$, and an estimated Doppler profile $\hat{Q}_{\mathbf{H}}(\nu) = \int_{\tau} |\hat{S}_{\mathbf{H}}(\tau, \nu)| d\tau$. The latter two functions are shown in Fig. 6. These quantities were used to derive the following channel parameters [see (8), (10), (12) with $|S_{\mathbf{H}}(\tau, \nu)|$ replaced by $|\hat{S}_{\mathbf{H}}(\tau, \nu)|$]: $\hat{\tau}_{\mathbf{H}}^{(1)} = 1.78 \mu\text{s}$, $\hat{\nu}_{\mathbf{H}}^{(1)} = 6.49$ Hz, and $\hat{\mu}_{\mathbf{H}}^{(1)} = 1.11 \times 10^{-5}$. With these channel parameter estimates and the sounder parameters specified further above, we obtained the upper error bounds $\varepsilon_1^{(1)} = 2.1 \cdot 10^{-3}$ (commutation error), $\varepsilon_2 = 9.76 \cdot 10^{-4}$ (pulse-compression error), $\varepsilon_3^{(1)} = 1.28$ (aliasing error), and $\varepsilon_4^{(1)} = 7 \cdot 10^{-5}$ (misinterpretation error). The bound $\varepsilon_1^{(1)}$ and ε_2 suggest that commutation error and pulse-compression error are well balanced. Indeed, the transmit/receive filter length used, $N = 1023$, equals N_{opt} as obtained from (51).

The large bound $\varepsilon_3^{(1)}$ suggests large aliasing errors. Since $\hat{\tau}_{\mathbf{H}}^{(1)} \ll T$, these aliasing errors cannot be due to an overlap of successive snapshots but must be due to the repetition rate

$1/T_{\text{rep}}$ being too small to properly track the channel's time variations. Indeed, $1/T_{\text{rep}} = 20.35$ Hz is quite close to the double mean Doppler shift $2\hat{\nu}_{\mathbf{H}}^{(1)} = 12.98$ Hz. The corresponding aliasing effects are also visible in the measured Doppler profile in Fig. 6(b). The aliasing error can be reduced by using a shorter sounding period T and/or a smaller repetition factor K . Setting for example $K = 1$, (52) yields the sounding period $T_{\text{opt}}^{(1)} = 370$ μs , which would reduce the aliasing error bound to about $\varepsilon_3^{(1)} \approx 0.02$ (i.e., by a factor of 64). However, this choice of K and T requires faster data acquisition.

Finally, the bound $\varepsilon_4^{(1)}$ suggests that compared to the other error components, the misinterpretation error is negligible. Thus, the measured channel snapshots can be used equally well as estimates of $h_{\mathbf{H}}^{\text{I}}(t, \tau)$ or $h_{\mathbf{H}}^{\text{O}}(t, \tau)$.

VIII. SUMMARY AND CONCLUSION

Based on a unified mathematical framework for (uncalibrated) channel sounders, we analyzed the systematic errors that arise in the sounding of time-varying mobile radio channels. We identified four different error components and developed upper bounds for each of them. These error bounds show that systematic measurement errors will be small if the channel is underspread and if the sounder parameters are properly chosen. The error bounds also lead to guidelines for a judicious choice of sounder parameters. Our theoretical results were illustrated by numerical simulations and their usefulness in assessing the accuracy of existing channel measurements was demonstrated. We note that an analysis of *calibrated* channel sounders and an improved calibration technique are presented in [7].

APPENDIX A

PROOF OF COMMUTATION ERROR BOUNDS

We shall first prove the error bound in (34). With (25) and (17), and assuming $T_g \leq T$, we have

$$\begin{aligned}
& |e_1(mT_{\text{rep}}, \tau)| \\
&= |([\mathbf{R}, \mathbf{H}]x)(\tau + mT_{\text{rep}})w(\tau)| \\
&\leq |([\mathbf{R}, \mathbf{H}]x)(\tau + mT_{\text{rep}})| \\
&= \left| \int_{\tau'} \int_{\nu} S_{[\mathbf{R}, \mathbf{H}]}^{\text{I}}(\tau', \nu) x(\tau + mT_{\text{rep}} - \tau') \right. \\
&\quad \left. \times e^{j2\pi\nu(\tau + mT_{\text{rep}})} d\tau' d\nu \right| \\
&\leq \int_{\tau'} \int_{\nu} |S_{[\mathbf{R}, \mathbf{H}]}^{\text{I}}(\tau', \nu)| |x(\tau + mT_{\text{rep}} - \tau')| d\tau' d\nu \\
&\leq \|x\|_{\infty} \int_{\tau'} \int_{\nu} |S_{[\mathbf{R}, \mathbf{H}]}^{\text{I}}(\tau', \nu)| d\tau' d\nu \\
&= \|g\|_{\infty} \|S_{[\mathbf{R}, \mathbf{H}]}^{\text{I}}\|_1 \tag{55}
\end{aligned}$$

where we used $|w(\tau)| \leq 1$, (7), and $\|x\|_{\infty} = \|g\|_{\infty}$ due to $T_g \leq T$. With the *twisted convolution* [12], [32]

$$\begin{aligned}
S_{\mathbf{H}_2\mathbf{H}_1}^{\text{I}}(\tau, \nu) &= \int_{\tau'} \int_{\nu'} S_{\mathbf{H}_2}^{\text{I}}(\tau', \nu') S_{\mathbf{H}_1}^{\text{I}}(\tau - \tau', \nu - \nu') \\
&\quad \times e^{j2\pi\tau'(\nu - \nu')} d\tau' d\nu' \tag{56}
\end{aligned}$$

and the fact that $S_{\mathbf{R}}^{\text{I}}(\tau, \nu) = r(\tau)\delta(\nu)$ since \mathbf{R} is time-invariant, $\|S_{[\mathbf{R}, \mathbf{H}]}^{\text{I}}\|_1$ can be bounded as follows:

$$\begin{aligned}
& \|S_{[\mathbf{R}, \mathbf{H}]}^{\text{I}}\|_1 \\
&= \int_{\tau} \int_{\nu} |S_{\mathbf{RH}}^{\text{I}}(\tau, \nu) - S_{\mathbf{HR}}^{\text{I}}(\tau, \nu)| d\tau d\nu \\
&= \int_{\tau} \int_{\nu} \left| \int_{\tau'} \int_{\nu'} r(\tau') \delta(\nu') S_{\mathbf{H}}^{\text{I}}(\tau - \tau', \nu - \nu') \right. \\
&\quad \times e^{j2\pi\tau'(\nu - \nu')} d\tau' d\nu' \\
&\quad \left. - \int_{\tau'} \int_{\nu'} S_{\mathbf{H}}^{\text{I}}(\tau', \nu') r(\tau - \tau') \delta(\nu - \nu') \right. \\
&\quad \left. \times e^{j2\pi\tau'(\nu - \nu')} d\tau' d\nu' \right| d\tau d\nu \\
&= \int_{\tau} \int_{\nu} \left| \int_{\tau'} r(\tau') S_{\mathbf{H}}^{\text{I}}(\tau - \tau', \nu) [e^{j2\pi\tau'\nu} - 1] d\tau' \right| d\tau d\nu \\
&\leq 2 \int_{\tau_1} \int_{\nu} \int_{\tau'} |r(\tau')| |S_{\mathbf{H}}^{\text{I}}(\tau_1, \nu)| |\sin(\pi\tau'\nu)| d\tau_1 d\nu d\tau' \\
&\leq 2\pi \int_{\tau} \int_{\nu} |S_{\mathbf{H}}^{\text{I}}(\tau, \nu)| |\nu| d\tau d\nu \int_{\tau'} |r(\tau')| |\tau'| d\tau' \\
&= 2\pi \|S_{\mathbf{H}}\|_1 \bar{\nu}_{\mathbf{H}}^{(1)} \|r\|_1 \bar{\tau}_{\mathbf{R}}^{(1)}. \tag{57}
\end{aligned}$$

Here, we used $|\sin x| \leq |x|$ and the definitions of $\bar{\tau}_{\mathbf{R}}^{(1)}$ and $\bar{\nu}_{\mathbf{H}}^{(1)}$. Inserting (57) in (55), we finally obtain (34),

$$|e_1(mT_{\text{rep}}, \tau)| \leq 2\pi \|g\|_{\infty} \|S_{\mathbf{H}}\|_1 \|r\|_1 \bar{\tau}_{\mathbf{R}}^{(1)} \bar{\nu}_{\mathbf{H}}^{(1)}.$$

Next, we prove the bound on $\int_{\tau} |e_1(t, \tau)| d\tau$ in (38), under the assumptions $(\Upsilon\mathbf{RHG}\Delta)(t, \tau) = h_{\mathbf{RHG}}^{\text{O}}(t, \tau)$ and $(\Upsilon\mathbf{HRG}\Delta)(t, \tau) = h_{\mathbf{HRG}}^{\text{O}}(t, \tau)$. With (25), this entails

$$\begin{aligned}
e_1(t, \tau) &= (\Upsilon\mathbf{RHG}\Delta)(t, \tau) - (\Upsilon\mathbf{HRG}\Delta)(t, \tau) \\
&= h_{\mathbf{RHG}}^{\text{O}}(t, \tau) - h_{\mathbf{HRG}}^{\text{O}}(t, \tau) \\
&= h_{[\mathbf{R}, \mathbf{H}]\mathbf{G}}^{\text{O}}(t, \tau) \\
&= \int_{\nu} S_{[\mathbf{R}, \mathbf{H}]\mathbf{G}}^{\text{O}}(\tau, \nu) e^{j2\pi\nu t} d\nu.
\end{aligned}$$

Using (56) and the fact that $S_{\mathbf{G}}^{\text{I}}(\tau, \nu) = g(\tau)\delta(\nu)$ since \mathbf{G} is time-invariant, we obtain

$$\begin{aligned}
& \int_{\tau} |e_1(t, \tau)| d\tau \\
&= \int_{\tau} \left| \int_{\nu} S_{[\mathbf{R}, \mathbf{H}]\mathbf{G}}^{\text{O}}(\tau, \nu) e^{j2\pi\nu t} d\nu \right| d\tau \\
&\leq \int_{\tau} \int_{\nu} |S_{[\mathbf{R}, \mathbf{H}]\mathbf{G}}^{\text{O}}(\tau, \nu)| d\tau d\nu \\
&= \int_{\tau} \int_{\nu} |S_{[\mathbf{R}, \mathbf{H}]\mathbf{G}}^{\text{I}}(\tau, \nu)| d\tau d\nu \\
&= \int_{\tau} \int_{\nu} \left| \int_{\tau'} \int_{\nu'} S_{[\mathbf{R}, \mathbf{H}]}^{\text{I}}(\tau', \nu') g(\tau - \tau') \delta(\nu - \nu') \right. \\
&\quad \left. \times e^{j2\pi\tau'(\nu - \nu')} d\tau' d\nu' \right| d\tau d\nu \\
&\leq \int_{\tau} \int_{\nu} |S_{[\mathbf{R}, \mathbf{H}]}^{\text{I}}(\tau, \nu)| d\tau d\nu \int_{\tau} |g(\tau)| d\tau \\
&\leq 2\pi \|S_{\mathbf{H}}\|_1 \bar{\nu}_{\mathbf{H}}^{(1)} \|r\|_1 \bar{\tau}_{\mathbf{R}}^{(1)} \|g\|_1
\end{aligned}$$

where in the last step we used the bound (57) on $\|S_{[\mathbf{R}, \mathbf{H}]}^{\text{I}}\|_1$. This completes the proof of (38).

APPENDIX B

PROOF OF PULSE-COMPRESSION ERROR BOUNDS

We first prove the bound (40). With (26), (17), $|w(\tau)| \leq 1$, and (3), we obtain

$$\begin{aligned} & |e_2(mT_{\text{rep}}, \tau)| \\ &= |(\mathbf{HRG}\Delta)(\tau+mT_{\text{rep}})w(\tau) - (\mathbf{H}\Delta)(\tau+mT_{\text{rep}})w(\tau)| \\ &\leq |(\mathbf{HRG}\Delta)(\tau+mT_{\text{rep}}) - (\mathbf{H}\Delta)(\tau+mT_{\text{rep}})| \\ &= \left| \int_f [L_{\mathbf{HRG}}^I(\tau+mT_{\text{rep}}, f) - L_{\mathbf{H}}^I(\tau+mT_{\text{rep}}, f)] \right. \\ &\quad \times \left. \left[\frac{1}{T} \sum_k \delta\left(f - \frac{k}{T}\right) \right] e^{j2\pi f(\tau+mT_{\text{rep}})} df \right|. \end{aligned}$$

Using that $L_{\mathbf{HRG}}^I(t, f) = L_{\mathbf{H}}^I(t, f)R(f)G(f)$ since \mathbf{G} and \mathbf{R} are time-invariant, that $L_{\mathbf{H}}^I(t, f) = 0$ for $f \notin [-B, B]$ due to the bandlimitation of \mathbf{H} [see Fig. 1(a)], and that $|L_{\mathbf{H}}^I(t, f)| \leq \|S_{\mathbf{H}}\|_1$, we further obtain

$$\begin{aligned} & |e_2(mT_{\text{rep}}, \tau)| \\ &\leq \left| \int_{-B}^B L_{\mathbf{H}}^I(\tau+mT_{\text{rep}}, f)[R(f)G(f) - 1] \right. \\ &\quad \times \left. \left[\frac{1}{T} \sum_k \delta\left(f - \frac{k}{T}\right) \right] e^{j2\pi(\tau+mT_{\text{rep}})f} df \right| \\ &= \left| \frac{1}{T} \sum_{|k| \leq BT} L_{\mathbf{H}}^I\left(\tau+mT_{\text{rep}}, \frac{k}{T}\right) \right. \\ &\quad \times \left. \left[R\left(\frac{k}{T}\right)G\left(\frac{k}{T}\right) - 1 \right] e^{j2\pi(\tau+mT_{\text{rep}})k/T} \right| \\ &\leq \frac{1}{T} \sum_{|k| \leq BT} \left| L_{\mathbf{H}}^I\left(\tau+mT_{\text{rep}}, \frac{k}{T}\right) \right| \\ &\quad \times \left| R\left(\frac{k}{T}\right)G\left(\frac{k}{T}\right) - 1 \right| \\ &\leq \|S_{\mathbf{H}}\|_1 \frac{1}{T} \sum_{|k| \leq BT} \left| R\left(\frac{k}{T}\right)G\left(\frac{k}{T}\right) - 1 \right| \end{aligned}$$

which is (40).

We next prove the bounds in (43) and (44). Assuming $(\mathbf{YHRG}\Delta)(t, \tau) = h_{\mathbf{HRG}}^O(t, \tau)$ and $(\mathbf{YH}\Delta)(t, \tau) = h_{\mathbf{H}}^O(t, \tau)$, we have $e_2(t, \tau) = h_{\mathbf{HRG}}^O(t, \tau) - h_{\mathbf{H}}^O(t, \tau)$. Let $S_{e_2}(\tau, \nu) \triangleq \mathcal{F}\{e_2(t, \tau)\} = S_{\mathbf{HRG}}^O(\tau, \nu) - S_{\mathbf{H}}^O(\tau, \nu)$, and recall that $|S_{e_2}^O(\tau, \nu)| = |S_{e_2}^I(\tau, \nu)|$. It then follows that

$$\begin{aligned} & \int_{\tau} |e_2(t, \tau)| d\tau \\ &= \int_{\tau} \left| \int_{\nu} S_{e_2}(\tau, \nu) e^{j2\pi\nu t} d\nu \right| d\tau \\ &\leq \int_{\tau} \int_{\nu} |S_{e_2}(\tau, \nu)| d\tau d\nu \\ &= \int_{\tau} \int_{\nu} |S_{\mathbf{HRG}}^I(\tau, \nu) - S_{\mathbf{H}}^I(\tau, \nu)| d\tau d\nu \\ &= \int_{\tau} \int_{\nu} \left| \int_{\tau'} S_{\mathbf{H}}^I(\tau - \tau', \nu) (r * g)(\tau') d\tau' - S_{\mathbf{H}}^I(\tau, \nu) \right| d\tau d\nu. \end{aligned}$$

Due to the bandlimitation of \mathbf{H} , there is $L_{\mathbf{H}}^I(t, f) = L_{\mathbf{H}}^I(t, f)\text{rect}_B(f)$ [where $\text{rect}_B(f)$ is 1 for $|f| \leq B$ and 0 otherwise]. Since $L_{\mathbf{H}}^I(t, f)$ and $S_{\mathbf{H}}^I(\tau, \nu)$ are related by a 2-D Fourier transform, this implies $S_{\mathbf{H}}^I(\tau, \nu) = S_{\mathbf{H}}^I(\tau, \nu) *_{\tau} \text{sinc}_B(\tau)$ with $\text{sinc}_B(\tau) \triangleq B \text{sinc}(\pi B\tau)$. Hence, we obtain

$$\begin{aligned} & \int_{\tau} |e_2(t, \tau)| d\tau \\ &\leq \int_{\tau} \int_{\nu} \left| \int_{\tau'} S_{\mathbf{H}}^I(\tau - \tau', \nu) (r * g * \text{sinc}_B)(\tau') d\tau' \right. \\ &\quad \left. - \int_{\tau'} S_{\mathbf{H}}^I(\tau - \tau', \nu) \text{sinc}_B(\tau') d\tau' \right| d\tau d\nu \\ &= \int_{\tau} \int_{\nu} \left| \int_{\tau'} S_{\mathbf{H}}^I(\tau - \tau', \nu) [(r * g * \text{sinc}_B)(\tau') \right. \\ &\quad \left. - \text{sinc}_B(\tau')] d\tau' \right| d\tau d\nu \\ &\leq \int_{\tau_1} \int_{\nu} \int_{\tau'} |S_{\mathbf{H}}^I(\tau_1, \nu)| \\ &\quad \times |(r * g * \text{sinc}_B)(\tau') - \text{sinc}_B(\tau')| d\tau_1 d\nu d\tau' \\ &= \|S_{\mathbf{H}}\|_1 \int_{\tau} |(r * g * \text{sinc}_B)(\tau) - \text{sinc}_B(\tau)| d\tau \end{aligned}$$

which is (43). The bound in (44) is obtained from (43) using (32).

Finally, we prove (45) and (46). With $L_{e_2}(t, f) = L_{\mathbf{HRG}}^O(t, f) - L_{\mathbf{H}}^O(t, f)$, $\|L_{e_2}^O\|_2 = \|L_{\mathbf{H}}^O\|_2$, and $L_{\mathbf{H}}^O(t, f) = 0$ for $|f| > B$, we obtain

$$\begin{aligned} & \|L_{e_2}\|_2 \\ &= \|L_{\mathbf{HRG}}^O - L_{\mathbf{H}}^O\|_2 = \|L_{\mathbf{HRG}}^I - L_{\mathbf{H}}^I\|_2 \\ &= \left[\int_t \int_{-B}^B |L_{\mathbf{H}}^I(t, f)R(f)G(f) - L_{\mathbf{H}}^I(t, f)|^2 dt df \right]^{1/2} \\ &= \left[\int_t \int_{-B}^B |L_{\mathbf{H}}^I(t, f)|^2 |R(f)G(f) - 1|^2 dt df \right]^{1/2} \\ &\leq \max_{f \in [-B, B]} |R(f)G(f) - 1| \left[\int_t \int_{-B}^B |L_{\mathbf{H}}^I(t, f)|^2 dt df \right]^{1/2} \\ &= \|L_{\mathbf{H}}^I\|_2 \max_{f \in [-B, B]} |R(f)G(f) - 1|. \end{aligned}$$

With $\|L_{\mathbf{H}}^I\|_2 = \|S_{\mathbf{H}}\|_2$, this yields (46). The bound in (45) follows from (46) using (33).

APPENDIX C

PROOF OF ALIASING ERROR BOUNDS

We first show the bound (47) on $e_3(t, \tau) = (\mathbf{YH}\Delta)(t, \tau) - h_{\mathbf{H}}^O(t, \tau)$ [cf. (28)]. With (17) and $(\mathbf{H}\Delta)(t) = \sum_n k_{\mathbf{H}}(t, nT) = \sum_n h_{\mathbf{H}}^O(nT, t - nT)$ [cf. (14)], we have

$$\begin{aligned} & \tilde{h}_{\mathbf{H}}^O(t, \tau) \triangleq (\mathbf{YH}\Delta)(t, \tau) \\ &= \sum_m (\mathbf{H}\Delta)(\tau+mT_{\text{rep}})w(\tau) \text{sinc}\left(\frac{\pi}{T_{\text{rep}}}(t-mT_{\text{rep}})\right) \\ &= \sum_m \left[\sum_n h_{\mathbf{H}}^O(nT, \tau+mT_{\text{rep}} - nT) \right] w(\tau) \\ &\quad \times \text{sinc}\left(\frac{\pi}{T_{\text{rep}}}(t-mT_{\text{rep}})\right). \end{aligned}$$

We then obtain the spreading function estimate

$$\begin{aligned}
\tilde{S}_{\mathbf{H}}^{\text{O}}(\tau, \nu) &\triangleq \int_t \tilde{h}_{\mathbf{H}}^{\text{O}}(t, \tau) e^{-j2\pi\nu t} dt \\
&= \int_t \left[\sum_m \sum_n h_{\mathbf{H}}^{\text{O}}(nT, \tau + mT_{\text{rep}} - nT) w(\tau) \right. \\
&\quad \left. \times \text{sinc}\left(\frac{\pi}{T_{\text{rep}}}(t - mT_{\text{rep}})\right) \right] e^{-j2\pi\nu t} dt \\
&= T_{\text{rep}} \sum_m \sum_n h_{\mathbf{H}}^{\text{O}}(nT, \tau + (mK - n)T) w(\tau) I(\nu) \\
&\quad \times e^{-j2\pi\nu mT_{\text{rep}}} \\
&= w(\tau) I(\nu) T_{\text{rep}} \sum_m \sum_k h_{\mathbf{H}}^{\text{O}}(mT_{\text{rep}} - kT, \tau + kT) \\
&\quad \times e^{-j2\pi\nu mT_{\text{rep}}} \\
&= I_{\mathcal{R}}(\tau, \nu) \sum_k \sum_l S_{\mathbf{H}}^{\text{O}}\left(\tau + kT, \nu + \frac{l}{T_{\text{rep}}}\right) \\
&\quad \times e^{-j2\pi k(\nu + (l/T_{\text{rep}}))T} \quad (58)
\end{aligned}$$

where $I(\nu)$ is the 1-D indicator function of $[-1/(2T_{\text{rep}}), 1/(2T_{\text{rep}})]$ and $I_{\mathcal{R}}(\tau, \nu) = w(\tau) I(\nu)$ is the 2-D indicator function of the region $\mathcal{R} = [0, T] \times [-1/(2T_{\text{rep}}), 1/(2T_{\text{rep}})]$. From (58), it follows that $\tilde{S}_{\mathbf{H}}^{\text{O}}(\tau, \nu) = S_{\mathbf{H}}^{\text{O}}(\tau, \nu)$ if and only if $S_{\mathbf{H}}^{\text{O}}(\tau, \nu)$ is completely contained within \mathcal{R} . The aliasing error can be described in the delay-Doppler domain by $S_{e_3}(\tau, \nu) \triangleq \mathcal{F}_{t \rightarrow \nu} \{e_3(t, \tau)\} = \tilde{S}_{\mathbf{H}}^{\text{O}}(\tau, \nu) - S_{\mathbf{H}}^{\text{O}}(\tau, \nu)$. Using (58), we obtain

$$\begin{aligned}
S_{e_3}(\tau, \nu) &= I_{\mathcal{R}}(\tau, \nu) \sum_k \sum_l S_{\mathbf{H}}^{\text{O}}\left(\tau + kT, \nu + \frac{l}{T_{\text{rep}}}\right) \\
&\quad \times e^{-j2\pi k(\nu + (l/T_{\text{rep}}))T} - S_{\mathbf{H}}^{\text{O}}(\tau, \nu) \\
&= \Delta S_1(\tau, \nu) + \Delta S_2(\tau, \nu)
\end{aligned}$$

with

$$\begin{aligned}
\Delta S_1(\tau, \nu) &\triangleq S_{\mathbf{H}}^{\text{O}}(\tau, \nu) [I_{\mathcal{R}}(\tau, \nu) - 1] \\
\Delta S_2(\tau, \nu) &\triangleq I_{\mathcal{R}}(\tau, \nu) \sum_{k \neq 0} \sum_{l \neq 0} S_{\mathbf{H}}^{\text{O}}\left(\tau + kT, \nu + \frac{l}{T_{\text{rep}}}\right) \\
&\quad \times e^{-j2\pi k(\nu + (l/T_{\text{rep}}))T}.
\end{aligned}$$

The component $\Delta S_1(\tau, \nu)$ is the error resulting from the suppression of spreading function components outside the region \mathcal{R} , corresponding to delays larger than T and Doppler frequencies with magnitudes larger than $1/(2T_{\text{rep}})$. The component $\Delta S_2(\tau, \nu)$ describes aliasing components falling into the region \mathcal{R} . With $\bar{\mathcal{R}}$ denoting the region complementary to \mathcal{R} , and noting that $|I_{\mathcal{R}}(\tau, \nu) - 1| = I_{\bar{\mathcal{R}}}(\tau, \nu)$, we have

$$\begin{aligned}
\|S_{e_3}\|_1 &\leq \|\Delta S_1\|_1 + \|\Delta S_2\|_1 \\
&= \int_{\tau} \int_{\nu} |S_{\mathbf{H}}^{\text{O}}(\tau, \nu)| I_{\bar{\mathcal{R}}}(\tau, \nu) d\tau d\nu \\
&\quad + \int_0^T \int_{-1/(2T_{\text{rep}})}^{1/(2T_{\text{rep}})} \left| \sum_{k \neq 0} \sum_{l \neq 0} S_{\mathbf{H}}^{\text{O}}\left(\tau + kT, \nu + \frac{l}{T_{\text{rep}}}\right) \right. \\
&\quad \left. \times e^{-j2\pi k(\nu + (l/T_{\text{rep}}))T} \right| d\tau d\nu
\end{aligned}$$

$$\begin{aligned}
&\leq \iint_{\bar{\mathcal{R}}} |S_{\mathbf{H}}^{\text{O}}(\tau, \nu)| d\tau d\nu \\
&\quad + \sum_{k \neq 0} \sum_{l \neq 0} \int_{kT}^{(k+1)T} \int_{(l-1/2)/T_{\text{rep}}}^{(l+1/2)/T_{\text{rep}}} |S_{\mathbf{H}}^{\text{O}}(\tau', \nu')| d\tau' d\nu' \\
&= 2 \iint_{\bar{\mathcal{R}}} |S_{\mathbf{H}}(\tau, \nu)| d\tau d\nu. \quad (59)
\end{aligned}$$

For $(\tau, \nu) \in \bar{\mathcal{R}}$, there is $|\tau - \tau_0| \geq T - \tau_0$ or $|\nu| \geq 1/2T_{\text{rep}}$ and thus (assuming $T - \tau_0 > 0$) $(|\tau - \tau_0|)/(T - \tau_0) + 2T_{\text{rep}}|\nu| \geq 1$. Hence, (59) yields

$$\begin{aligned}
\|S_{e_3}\|_1 &\leq 2 \int_{\tau} \int_{\nu} \left[\frac{|\tau - \tau_0|}{T - \tau_0} + 2T_{\text{rep}}|\nu| \right] |S_{\mathbf{H}}(\tau, \nu)| d\tau d\nu \\
&= 2\|S_{\mathbf{H}}\|_1 \left[\frac{\bar{\tau}_{\mathbf{H}}^{(1)}}{T - \tau_0} + 2T_{\text{rep}}\bar{\nu}_{\mathbf{H}}^{(1)} \right].
\end{aligned}$$

With $\int_{\tau} |e_3(t, \tau)| d\tau \leq \|S_{e_3}\|_1$, this finally establishes the bound (47).

To show the bound (48), we note that

$$\begin{aligned}
\|\Delta S_1\|_2^2 &= \int_{\tau} \int_{\nu} |S_{\mathbf{H}}^{\text{O}}(\tau, \nu)|^2 I_{\bar{\mathcal{R}}}^2(\tau, \nu) d\tau d\nu \\
&= \iint_{\bar{\mathcal{R}}} |S_{\mathbf{H}}(\tau, \nu)|^2 d\tau d\nu
\end{aligned}$$

and

$$\begin{aligned}
\|\Delta S_2\|_2^2 &= \int_{\tau} \int_{\nu} \left| I_{\mathcal{R}}(\tau, \nu) \sum_{k \neq 0} \sum_{l \neq 0} S_{\mathbf{H}}^{\text{O}}\left(\tau + kT, \nu + \frac{l}{T_{\text{rep}}}\right) \right. \\
&\quad \left. \times e^{-j2\pi k(\nu + (l/T_{\text{rep}}))T} \right|^2 d\tau d\nu \\
&= \int_{\tau} \int_{\nu} \left| \sum_{k \neq 0} \sum_{l \neq 0} I_{\mathcal{R}}\left(\tau' - kT, \nu' - \frac{l}{T_{\text{rep}}}\right) \right. \\
&\quad \left. \times S_{\mathbf{H}}^{\text{O}}(\tau', \nu') e^{-j2\pi k\nu'T} \right|^2 d\tau' d\nu' \\
&\leq \int_{\tau} \int_{\nu} \left[\sum_{k \neq 0} \sum_{l \neq 0} I_{\mathcal{R}}\left(\tau' - kT, \nu' - \frac{l}{T_{\text{rep}}}\right) \right. \\
&\quad \left. \times |S_{\mathbf{H}}(\tau', \nu')| \right]^2 d\tau' d\nu' \\
&= \int_{\tau} \int_{\nu} [I_{\bar{\mathcal{R}}}(\tau', \nu') |S_{\mathbf{H}}(\tau', \nu')|]^2 d\tau' d\nu' \\
&= \iint_{\bar{\mathcal{R}}} |S_{\mathbf{H}}(\tau, \nu)|^2 d\tau d\nu.
\end{aligned}$$

Hence, we obtain

$$\begin{aligned}
\|e_3\|_2 &= \|S_{e_3}\|_2 \leq \|\Delta S_1\|_2 + \|\Delta S_2\|_2 \\
&\leq 2 \left[\iint_{\bar{\mathcal{R}}} |S_{\mathbf{H}}(\tau, \nu)|^2 d\tau d\nu \right]^{1/2} \\
&\leq 2 \left[\int_{\tau} \int_{\nu} \left[\frac{(\tau - \tau_0)^2}{(T - \tau_0)^2} + (2T_{\text{rep}}\nu)^2 \right] |S_{\mathbf{H}}(\tau, \nu)|^2 d\tau d\nu \right]^{1/2} \\
&= 2\|S_{\mathbf{H}}\|_2 \left[\left(\frac{\bar{\tau}_{\mathbf{H}}^{(2)}}{T - \tau_0} \right)^2 + \left(2T_{\text{rep}}\bar{\nu}_{\mathbf{H}}^{(2)} \right)^2 \right]^{1/2}.
\end{aligned}$$

ACKNOWLEDGMENT

The authors thank Prof. E. Bonek for his support and encouragement as well as for critical reading of the manuscript, and H. Artés for assistance with the simulations.

REFERENCES

- [1] T. S. Rappaport, *Wireless Communications: Principles & Practice*. Upper Saddle River, NJ: Prentice-Hall, 1996.
- [2] A. F. Molisch, Ed., *Wideband Wireless Digital Communications*. Upper Saddle River, NJ: Prentice-Hall, 2000.
- [3] J. D. Parsons, *The Mobile Radio Propagation Channel*. London, U.K.: Pentech, 1992.
- [4] J. D. Parsons, D. A. Demery, and A. M. D. Turkmani, "Sounding techniques for wideband mobile radio channels: A review," *Proc Inst. Elect. Eng.—I*, vol. 138, pp. 437–446, Oct. 1991.
- [5] P. J. Cullen, P. C. Fannin, and A. Molina, "Wide-band measurement and analysis techniques for the mobile radio channel," *IEEE Trans. Veh. Technol.*, vol. 42, pp. 589–603, Nov. 1993.
- [6] P. C. Fannin, A. Molina, S. S. Swords, and P. J. Cullen, "Digital signal processing techniques applied to mobile radio channel sounding," *Proc Inst. Elect. Eng.—F*, vol. 138, pp. 502–508, Oct. 1991.
- [7] G. Matz, A. F. Molisch, M. Steinbauer, F. Hlawatsch, I. Gaspard, and H. Artés, "Bounds on the systematic measurement errors of channel sounders for time-varying mobile radio channels," in *Proc. IEEE VTC-99 Fall*, Amsterdam, The Netherlands, Sept. 1999, pp. 1465–1470.
- [8] P. A. Bello, "Characterization of randomly time-variant linear channels," *IEEE Trans. Commun. Syst.*, vol. COM-11, pp. 360–393, 1963.
- [9] L. A. Zadeh, "Frequency analysis of variable networks," *Proc. IRE*, vol. 76, pp. 291–299, Mar. 1950.
- [10] W. Kozek, "On the generalized Weyl correspondence and its application to time-frequency analysis of linear time-varying systems," in *Proc. IEEE SP Int. Symp. Time-Freq. Time-Scale Analysis*, Victoria, Canada, Oct. 1992, pp. 167–170.
- [11] —, "On the transfer function calculus for underspread LTV channels," *IEEE Trans. Signal Processing*, vol. 45, pp. 219–223, Jan. 1997.
- [12] G. Matz and F. Hlawatsch, "Time-frequency transfer function calculus (symbolic calculus) of linear time-varying systems (linear operators) based on a generalized underspread theory," *J. Math. Phys., Special Issue on Wavelet and Time-Frequency Analysis*, vol. 39, pp. 4041–4071, Aug. 1998.
- [13] W. Kozek, "Matched Weyl–Heisenberg expansions of nonstationary environments," Ph.D. dissertation, Vienna Univ. Technol., Vienna, Austria, Mar. 1997.
- [14] G. Matz, "A time-frequency calculus for time-varying systems and nonstationary processes with applications," Ph.D. dissertation, Vienna Univ. Technol., Nov. 2000.
- [15] G. Matz and F. Hlawatsch, "Time-frequency transfer function calculus of linear time-varying systems," in *Time-Frequency Signal Analysis and Processing*, B. Boashash, Ed. Englewood Cliffs, NJ: Prentice-Hall, to be published.
- [16] P. E. Green, Jr., "Radar measurements of target scattering properties," in *Radar Astronomy*, J. V. Evans and T. Hagfors, Eds. New York: McGraw-Hill, 1968, ch. 1.
- [17] R. S. Kennedy, *Fading Dispersive Communication Channels*. New York: Wiley, 1969.
- [18] H. L. Van Trees, *Detection, Estimation, and Modulation Theory, Part III: Radar–Sonar Signal Processing and Gaussian Signals in Noise*. Malabar, FL: Krieger, 1992.
- [19] J. G. Proakis, *Digital Communications*, 3rd ed. New York: McGraw-Hill, 1995.
- [20] T. Kailath, "Measurements on time-variant communication channels," *IEEE Trans. Inform. Theory*, vol. 8, pp. 229–236, Sept. 1962.
- [21] S. H. Nawab and T. F. Quatieri, "Short-time Fourier transform," in *Advanced Topics in Signal Processing*, J. S. Lim and A. V. Oppenheim, Eds. Englewood Cliffs, NJ: Prentice-Hall, 1988, ch. 6, pp. 289–337.
- [22] T. Felhauer, P. Baier, W. König, and W. Mohr, "Optimum spread spectrum signals for wideband channel sounding," *Electron. Lett.*, vol. 29, pp. 563–564, Mar. 1993.
- [23] Y. Han, "On the minimization of overhead in channel impulse response measurement," *IEEE Trans. Veh. Technol.*, vol. 47, pp. 631–637, May 1998.
- [24] A. Molina and P. C. Fannin, "Application of mismatched filter theory to bandpass impulse response measurements," *Electron. Lett.*, vol. 29, pp. 162–163, Jan. 1993.
- [25] K. Schwarz, U. Martin, and H. W. Schüßler, "Devices for propagation measurements in mobile radio channels," in *Proc. IEEE PIMRC-93*, 1993, pp. 387–391.
- [26] R. Thomä, D. Hampicke, A. Richter, G. Sommerkorn, A. Schneider, U. Trautwein, and W. Wirnitzer, "Identification of time-variant directional mobile radio channels," *IEEE Trans. Instrum. Meas.*, vol. 49, pp. 357–364, Apr. 2000.
- [27] D. Cox, "Delay Doppler characteristics of multipath propagation in a suburban mobile radio environment," *IEEE Trans. Antennas Propagat.*, vol. 20, pp. 625–635, 1972.
- [28] S. Salous, N. Nikandrou, and N. Bajj, "Digital techniques for mobile radio chirp sounders," *Proc Inst. Elect. Eng. Commun.*, vol. 145, pp. 191–196, June 1998.
- [29] M. Skolnik, *Radar Handbook*. New York: McGraw-Hill, 1984.
- [30] A. W. Naylor and G. R. Sell, *Linear Operator Theory in Engineering and Science*, 2nd ed. New York: Springer, 1982.
- [31] W. Kozek and H. G. Feichtinger, "Time-frequency structured decorrelation of speech signals via nonseparable Gabor frames," in *Proc. IEEE ICASSP-97*, Munich, Germany, Apr. 1997, pp. 1439–1442.
- [32] G. B. Folland, *Harmonic Analysis in Phase Space*. Princeton, NJ: Princeton Univ. Press, 1989, vol. 122.



Gerald Matz (S'95–M'00) received the Diplom-Ingenieur and Dr.techn. degrees in electrical engineering from the Vienna University of Technology, Vienna, Austria, in 1994 and 2000, respectively.

Since 1995, he has been with the Department of Communications and Radio-Frequency Engineering, Vienna University of Technology. His research interests include wireless communications, statistical signal processing, and time-frequency signal processing.



Andreas F. Molisch (S'89–M'95–SM'00) received the Dipl.Ing., Dr.techn., and habilitation degrees from the Technical University Vienna (TU Vienna), Vienna, Austria, in 1990, 1994, and 1999, respectively.

From 1991 to 2001, he was with the Institut für Nachrichtentechnik und Hochfrequenztechnik (INTHFT) of the TU Vienna, becoming an Associate Professor there in 1999. From 1999 to 2000, he was on leave at the FTW Research Center for Telecommunications Vienna. Since March 2001, he has been with the Wireless Systems Research Department, AT&T Laboratories Research, Middletown, NJ. He has done research in the areas of SAW filters, radiative transfer in atomic vapors, atomic line filters, and base station antennas. His current research interests are the measurement and modeling of mobile radio channels, MIMO systems, smart antennas, and wideband wireless systems. He has authored, coauthored, or edited two books, five book chapters, approximately 45 journal papers, and numerous conference contributions.

Dr. Molisch is an editor of the IEEE JOURNAL ON SELECTED AREAS IN COMMUNICATIONS Wireless Series and co-editor of an upcoming special issue on MIMO and smart antennas in the *J. Wireless Comm. Mob. Comp.* He has participated in the European research initiatives "COST 231" and "COST 259" as Austrian representative. He has also been session organizer, session chairman, and member of the Program Committee of various international conferences. He is a member of ÖVE and VDE. He received the GiT prize in 1991, the Kardinal Innitzer prize in 1999, and an INGVAR award in 2001.



Franz Hlawatsch (S'85–M'88–SM'00) received the Diplom-Ingenieur, Dr.techn., and Univ.-Dozent degrees in electrical engineering/signal processing from the Vienna University of Technology, Austria, in 1983, 1988, and 1996, respectively.

Since 1983, he has been with the Institute of Communications and Radio-Frequency Engineering, Vienna University of Technology. During 1991–1992, he spent a sabbatical year with the Department of Electrical Engineering, University of Rhode Island. He has held Visiting

Professor positions with INP/ENSEEIH T Toulouse, France, in 1999 and 2001 and with IRCCyN/University of Nantes, France, in 2000. He authored the book *Time-Frequency Analysis and Synthesis of Linear Signal Spaces—Time-Frequency Filters, Signal Detection and Estimation, and Range-Doppler Estimation* (Boston: Kluwer, 1998) and coedited the book *The Wigner Distribution—Theory and Applications in Signal Processing* (Amsterdam, The Netherlands: Elsevier, 1997). He is currently coediting the book *Temps-Fréquence: Concepts et Outils* (Paris, France: Hermès). His research interests are in signal processing with emphasis on time–frequency methods and wireless communications applications.



Martin Steinbauer (S'99) was born in Vienna, Austria, in 1973. In 1996, he received the Dipl.-Ing. degree from Technische Universität Wien (TU Wien) with distinction.

From this time on he has been with the Institut für Nachrichtentechnik und Hochfrequenztechnik (INTHF) at TU Wien as a research engineer. During his three-year participation in the EU project METAMORP, he was occupied with radio channel measurement and characterization. As chairman of a subgroup on directional channel modeling within the European research initiative COST 259, he promoted harmonization among different channel modeling approaches toward a common concept and parameter setting for directional channel simulations. Correspondingly, his main interests are in a comprehensive characterization of the mobile radio propagation channel together with all aspects needed to achieve this, including appropriate measurement techniques and data evaluation methods.

Mr. Steinbauer is a student member of the Austrian Electrical Engineering Society.



Ingo Gaspard received the Dipl.-Ing. (M.Sc.) degree in electrical engineering from University of Kaiserslautern, Germany, in 1990.

After five years with T-Mobil Headquarters, Bonn, Germany, working in the area of validation and network management of their GSM network, he joined the Wide Area Radio Networks Group at the former research center of Deutsche Telekom AG, Darmstadt, now T-Nova (a subsidiary of DTAG) in 1996. There, he is currently involved in radio channel modeling, as well as in OFDM system and network simulation and optimization. He holds four patents/patents pending and has published more than 20 national/international conference papers.